Universidade de Aveiro
2014
Departamento de Engenharia de Materiais e Cerâmica

Andisheh Motealleh

Chitosan-FastOs®BG Membrane-Guides for Nervous Tissue Regeneration

Universidade de Aveiro
2014

Departamento de Engenharia de Materiais e Cerâmica

Andisheh Motealleh

Chitosan-FastOs®BG Membrane-Guides for Nervous Tissue Regeneration

Dissertation presented to the University of Aveiro in the fulfillment of the requirement for the awarding of the Masters in Materials and Biomedical Devices carried out under the supervision of Prof. José M. F. Ferreira, Associate Professor in the Department of Materials and Ceramic Engineering at the University of Aveiro, Dr. Alexandra Lemos, Post-dococtoral Researcher in the Department of Materials Science and Engineering at the University of Aveiro, and Prof. Ana Colette Maurício, Associate Professor in the Department of Veterinary Clinics at the University of Porto.

O júri / The jury

Presidente / President

Professor Doutor Francisco Manuel Lemos Amado
Universidade de Aveiro, Escola Superior de Saúde

Vogais / Committee

Professor Doutor José Maria da Fonte Ferreira
Universidade de Aveiro, Departmento Engenharia de Materials e Cerâmica (Orientador)

Doutora Bárbara Joana Martins Leite Ferreira
Universidade de Aveiro, Departmento de Química

Acknowledgments

I would first like to thank my supervisor Prof. José M.F. Ferreira for his guidance and support throughout the entire span of my project. A special thanks to Dr. Alexandra Lemos and to Prof. Ana Colette Maurício, my co-supervisors, for their patience to assist me with this project.

I would also like to acknowledge and thank all the members of our laboratory especially my wonderful friends Dr. Susana Olhero, Avito Rebelo, Saurabh Kapoor, Ana Catarina Fernandes and Filipa Correia for their friendship and assistance during my time in Aveiro.

Dedications

This thesis is dedicated to my loving family, who offered me unconditional love, support and encouragement throughout the years. I will always appreciate my sister for helping me throughout the entire master program.

Abstract

Three-dimensional (3D) biodegradable composite porous scaffolds made of a biopolymer matrix (chitosan) and a bioactive glass (FastOs®BG-Z4) were fabricated via freeze drying as guides for nerve tissue engineering applications. For this purpose, chitosan was dissolved in aqueous solutions of lactic acid (LA, 1 wt.%) to reach a final concentration of 2 wt.%. Subsequently FastOs®BG-Z4 in powder form was added to chitosan solution in a chitosan/Fasto®BG-Z4 weight ratio of 50/50. The Chitosan/FastOs®BG-Z4 systems were cross-linked via adding different concentrations (0.01, 0.05 and 0.5 wt.%) of two kinds of cross-linking agents, genipin, a natural component, and glutaraldehyde, a synthetic agent, to stiffen the chitosan network. The final mixtures were then frozen at two temperatures, –20ºC and –80ºC followed by freeze-drying to obtain porous scaffolds.

For achieving the optimal Chitosan/FastOs®BG-Z4 scaffolds, the influences of adding FastOs®BG-Z4 powder and/or different amounts of crosslinking agents on the rheological properties of chitosan/LA solutions were firstly investigated by rheological measurements. The results showed that a strong and stable gel could not be obtained even when the highest amount of cross-linking agents (0.5 wt.%) was added to the 2 wt.% chitosan solution, while effective cross-linking occurred in the presence of FastOs®BG-Z4 powder. Therefore, it was concluded that FastOs®BG-Z4 plays an active role on chitosan complexation. The positive interactions between chitosan and the surface of FastOs®BG-Z4 particles and/or the ionic species leached out to the solution needs to be further investigated in future work.

The microstructural features of porous scaffolds were investigated by scanning electron microscope (SEM), and the porosity assessment was made by ethanol replacement method. The mechanical properties of porous scaffolds were investigated under compression/swelling tests with samples immersed in phosphate-buffered saline (PBS) solution. *In vitro* degradation tests were also performed by immersing the samples in

phosphate-buffered saline (PBS) solution for 2 months tests and the degradation degree was evaluated through the undergone weight changes.

The results showed some common features among genipin or glutaraldehyde as cross-linking agents: increasing their amounts from 0.01 to 0.5 wt.% led to reductions in gelling time, porosity fraction, swelling and degradation rate, while cross-linking degree increased. However, their effects on pore size and compression strength of the scaffolds diverged. For genipin pore size decreased and consequently the compression strength increased, while for glutaraldehyde pore size always increased with added amounts, but compression strength was improved with concentration increasing from 0.01 to 0.05 wt.%, decreasing when the added amount was further increased to 0.5 wt.%.

Moreover, –20ºC was selected as the most suitable freezing temperature when considering the porous microstructural features and the intended applications.

Resumo

A presente tese relata acerca do fabrico e caracterização de compósitos porosos tridimensionais (3D) biodegradáveis baseados em quitosano, como matriz biopolimérica, carregada com partículas de um vidro bioativo (Fastos®BG-Z4). Para este efeito, o quitosano foi dissolvido em solução aquosa de ácido láctico (LA, 1% em peso) até atingir uma concentração final de 2% em peso. Subsequentemente o Fastos®BG-Z4 em forma de pó foi adicionado à solução de quitosano em uma proporção em peso de quitosano/ Fastos®BG-Z4 de 50/50. Os sistemas quitosano/Fastos®BG-Z4 foram reticulados por meio de adição de diferentes percentagens em peso (0.01, 0.05 e 0.5) de dois tipos de agentes de ligação cruzada, um componente natural, genipin, e um agente sintético, glutaraldeído. As misturas finais foram então reticuladas a 60ºC seguido de congelamento a duas temperaturas diferentes, −20ºC e −80ºC. O gelo foi depois sublimado por liofilização de modo a obter matrizes porosas para aplicações como guias em engenharia de tecidos nervosos periféricos.

Com vista à optimização do processo de fabrico e das propriedades das estruturas porosas de suporte (andaimes) de quitosano/Fastos®BG-Z4, estudaram-se os efeitos da adição do Fastos®BG-Z4 em pó e/ou de diferentes quantidades de agentes de reticulação nas propriedades reológicas das soluções de LA/quitosano. Os resultados mostraram a impossibilidade de obter de um gel de quitosano suficientemente forte e estável mesmo quando a quantidade mais elevada de agentes de reticulação (0.5% em peso) foi adicionada à solução de quitosano, em contraste com o que aconteceu com a adição do pó de Fastos®BG-Z4 na ausência de outros agentes de reticulação. Esta descoberta permitiu concluir que o Fastos®BG-Z4 desempenha um papel activo na complexação do quitosano. As interacções positivas entre o quitosano e a superfície das partículas do Fastos®BG-Z4 e/ou as espécies iónicas lixiviadas para a solução precisam de ser melhor investigadas no futuro.

As características microestruturais dos materiais porosos foram investigadas por microscopia electrónica de varrimento (SEM), e a porosidade foi determinada pelo método de substituição de etanol. As propriedades mecânicas dos compósitos porosos imersos em solução (PBS) de solução salina tamponada com fosfato foram investigadas através de testes de compressão/inchamento. Realizaram-se também testes de degradação *in vitro* por imersão das amostras na mesma solução de PBS durante 2 meses, e o grau de degradação foi avaliado através das alterações de peso sofridas pelas amostras.

Os resultados mostraram algumas características comuns entre o genipin e o glutaraldeído como agentes de reticulação: o aumento das quantidades adicionadas (0.01–0.5% em peso) levou a reduções no tempo de gelificação, na fracção de porosidade, no grau de inchamento, e na taxa de degradação, enquanto o grau de reticulação aumentou. No entanto, os seus efeitos sobre o tamanho dos poros e a resistência à compressão dos suportes porosos divergiram. O tamanho de poro diminuiu no caso do genipin, o que se traduziu em consequentes aumentos da resistência à compressão; enquanto o tamanho dos poros aumentou sempre com as quantidades adicionadas no caso do glutaraldeído, pelo que só foram registadas melhorias na resistência à compressão na gama de concentrações entre 0.01–0.05% em peso, diminuindo quando a quantidade adicionada foi aumentada para 0,5 % em peso.

Verificou-se ainda que a temperatura de –20ºC era a que permitia obter as microestruturas porosas mais adequadas para as aplicações almejadas.

Table of Contents

List of Figures

List of Tables

List of Symbols and Abbreviations

Extracellular Matrix (ECM)

Central Nervous System (CNS)

Peripheral Nervous System (PNS)

Nerve Tissue Engineering (NTE)

Nerve Guidance Conduit (NGC)

Small Intestinal Submucosa (SIS)

Poly(lactic acid) (PLA)

Poly(lactic-co-glycolic acid) (PLGA)

Polysialic Acid (PSA)

Polyglycolic Acid (PGA)

Hydroxyapatite (HA)

Calcium Ion (Ca^{2+})

Zinc (Zn^{2+})

Diopside ($CaMgSi_2O_6$)

Fluorapatite ($Ca5(PO4)_3F$)

TCP ($3CaO.P_2O_5$)

Glutaraldehyde (GT)

Genipin (GP)

Solid Freeform Fabrication (SFF)

X-ray diffraction (XRD)

FastOs®BG-Z4 (F)

Lactic Acid (LA)

Deacetylation degree (DD)

Chitosan/FastOs®BG-Z4 (GP00/GT00)

Elastic Modulus (G′)

Viscous Modulus (G″)

Non-bridging Oxygens (NBOs)

Fourier Transform Infrared Spectroscopy-Attenuated Total Reflectance (FTIR-ATR)

Scanning Electron Microscopy (SEM)

Cross-linking Degree (CD)

Ninhydrin (NHN)

Equivalent circle diameter (ECD)

Phosphate Buffered Saline Solution (PBS)

Swelling Ratio (SR)

Bioglass (BG)

Non-bridging Oxygens (NBOs)

Amino (NH_2)

Elastic Modulus (E)

Weight Loss (WL)

Lactic Acid (LA)

Chapter 1

Introduction

1.1 Tissue Engineering

Nowadays, the tissues and/or organs for transplantation mainly come from donations which, however, cannot meet the clinical needs as a result of several shortcomings of this treatment such as longer operation to remove tissue from the donor site, the quality and quantity of tissue available for grafting, the risk of immune response and the transmission of viral and prionic diseases and infections from the donor, as well as the insufficient number of suitable donors available. In some cases permanent prostheses may be used to restore partial function to the injured organ. However, the artificial nature of prostheses causes several problems, which are considered to be of less importance in comparison to regeneration of the injured organ. In order to overcome the limitations of transplantation and prosthesis, a new interdisciplinary field called tissue engineering was greatly developed and artificial tissues and organs have been fabricated in vitro along the last two decades [1] [2].

The first tissue engineering definition was made in 1988 at National Science Foundation meeting as “The application of the principles and methods of engineering and the life science toward the fundamental understanding of structure-function relationships in normal and pathological mammalian tissue and the development of biological substitutes to restore, maintain or improve functions” [3]. The innovative approach of tissue engineering is to seed isolated cells with tissue inducing substances, such as growth and differentiation factors, on a scaffold which mimics the extracellular matrix (ECM) and acts as a cell attachment, proliferating, migrating and functioning environment (Figure 1.1) [3].

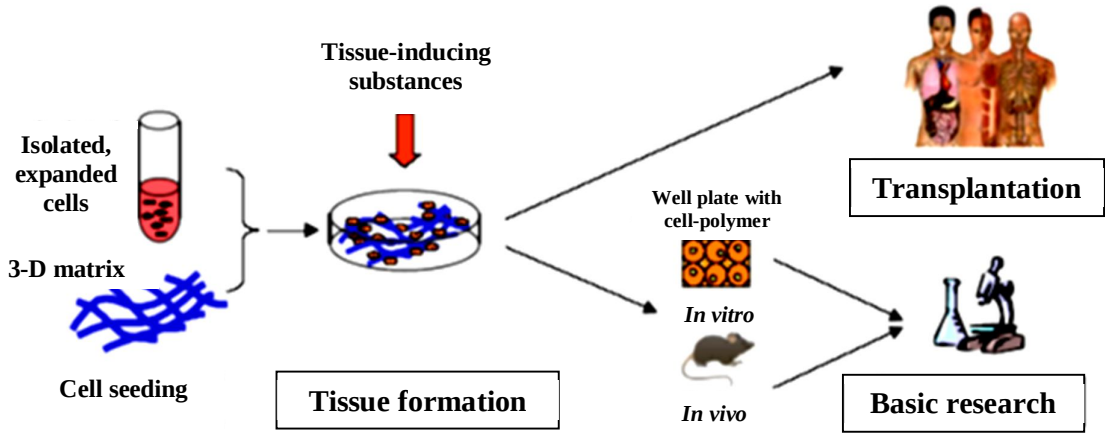

Figure 1.1. Diagram of tissue engineering approach [3].

One of the principal methods in tissue engineering involves the use of porous scaffolds to support and guide the in-growth of cells. Tissue scaffolds must be biocompatible, biodegradable, bioresorbable, and sterilizable. The scaffold must provide a number of properties and functionalities, including: (i) enough mechanical strength in order to facilitate *in vitro* handling and withstand the *in vivo* environment; (ii) sustaining cell function and provide an environment suitable for cellular growth; (iii) contain suitable surface properties (wettability, stiffness, and compliance) to support cell attachment, proliferation and differentiation. The degradation products should be biocompatible, non-toxic, and transportable out of the body [4]. Additionally, the pore architecture of scaffolds has been shown to have a significant effect on physical properties and cellular activities. It has been hypothesized that the pore diameter must be large enough to allow infiltration of the cells towards the centre of the scaffold, whilst being small enough to present sufficient ligand density for cellular attachment. The optimal pore size is dependent on both the cell type and scaffold material [2]. Lee [5] proposed a minimum pore size of 150 μm for hard tissue and 200–250 μm for soft tissue ingrowth.

1.2 Objectives

The aims of this project are (a) developing 3D biodegradable composite porous scaffolds made of chitosan and bioactive glass (FastOs®BG-Z4) as guides for peripheral nervous tissue regeneration; (b) microstructural and mechanical characterization of the prepared scaffolds. For this purpose, Chitosan was dissolved in aqueous solutions of lactic acid (LA) to which powdered FastOs®BG-Z4 bioactive glass was added together with different amounts of crosslinking agents (glutaraldehyde and genipin) to reticulate the chitosan. The final mixtures were reticulated at suitable temperature and then frozen at two different temperatures (–20ºC and –80ºC) followed by freeze-drying to obtain porous scaffolds.

For achieving the optimal chitosan/FastOs®BG-Z4 scaffolds, the dependence of the rheological properties of chitosan/LA solutions with fixed chitosan/FastOs®BG-Z4 ratio (50:50) and different amounts of cross-linking agents (0.01, 0.05, 0.5 wt.% related to the dry weight of chitosan) will be firstly investigated. The effects of cross-linking agents and their concentrations on gelation time, and on the physical and structural features of scaffolds (pore size, pore size distribution, compressive strength, swelling and degradation behaviours) will be investigated.

1.3 Thesis Outline

This dissertation consists of six chapters. The present chapter gives a short general introduction to the theme, presents the main objectives of this research work, and outlines the content of the different parts of the document. The second chapter gives a detailed account about the state of the arte in this specific area of human nervous system, nerve injuries and regeneration materials/approaches. The starting materials and reagents, the experimental procedures used in the fabrication of the polymeric/composite 3D porous scaffolds and for assessment their relevant properties are described in chapter 3. The experimental results obtained are presented and discussed in chapter 4. Chapter 5 summarises the findings and the main conclusions that could be drawn from all experiments. Chapter 6 indicates research directions to further explore the most exciting aspects of the present work. Finally, the document ends with a list of updated bibliographic references cited along the text.

Chapter 2

State of The Art

2.1 Nerve Tissue, Injuries and Regeneration

The human nervous system is classified into two systems, central nervous system (CNS) and the peripheral nervous system (PNS). The CNS includes the brain, spinal cord, optic, olfactory and auditory systems. Peripheral nerves are cord-like structures containing bundles of nerve fibres that carry information from regions of the body to the spinal cord (and vice versa). Peripheral nerves have a tough outer layer of connective tissue that surrounds discrete groups of miniscule fibres, called “axons,” each originating from its own nerve cell (Figure 2.1) [6] [7].

Endoneurium surrounds individual axons and their Schwann cell sheaths and is composed predominantly of oriented collagen fibres. Next, the perineurium, formed from many layers of flattened cells (i.e., fibroblasts) and collagen, surrounds groups of axons to form fascicles. Finally, epineurium, an outer sheath of loose fibrocollagenous tissue, binds individual nerve fascicles into a nerve trunk [6] [7].

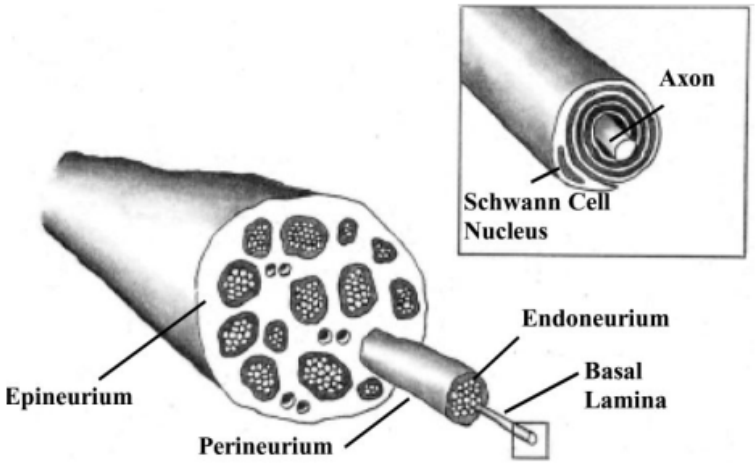

Figure 2.1. Anatomical overview of the PNS [6].

The spinal cord is composed of dendrites, axons, and cell bodies (Figure 2.2). The centre of the spinal cord, a butterfly-shaped region referred to as grey matter, contains the cell bodies of excitatory neurons, as well as glial cells and blood vessels. The grey matter is surrounded by white matter, which helps to protect and insulate the spinal cord. White matter consists of axons and glial cells [6] [7].

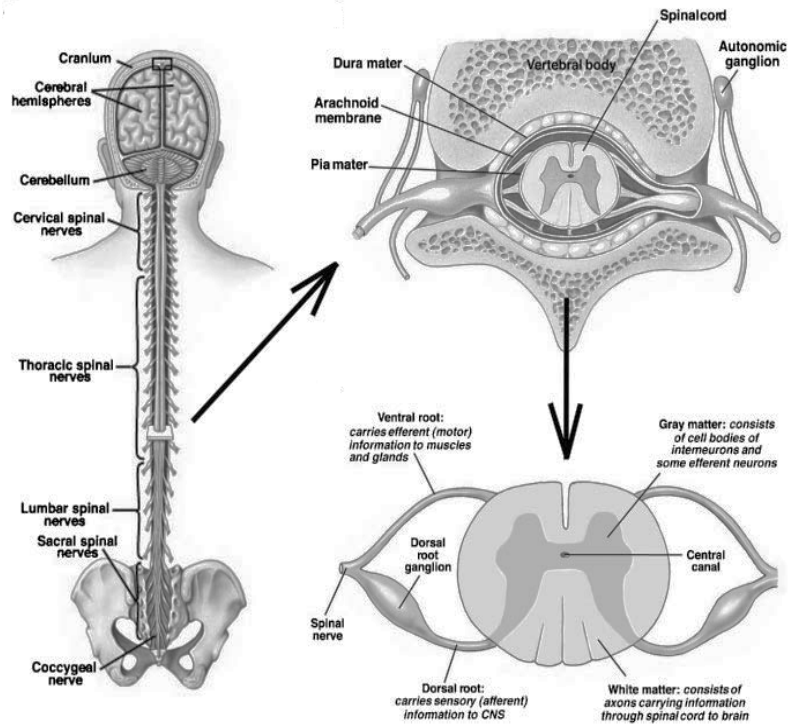

Figure 2.2. Figure Anatomy overview of the spinal cord [1].

Injuries in the central nervous system have only a very limited capacity to heal, because nerve regeneration tends not to occur. In contrast, peripheral nerves have a remarkable capacity for regeneration. Even completely severed peripheral nerves, if repaired promptly, can regrow, allowing the patients to enjoy complete or nearly complete recovery in many cases [6] [7].

Peripheral nerves are fragile and easily damaged. A peripheral nerve, when severed, is capable of a significant amount of regeneration. Peripheral nerves are discrete trunks filled

with sensory and motor axons, and support a number of cell types, such as Schwann cells and fibroblasts [6] [7]. The peripheral nerve trunk can be considered as a protective structure for axons. The most popular approach in peripheral nerve tissue engineering involves *in vivo* implantation of artificial scaffolds and substrates that will guide naturally regenerating axons to the distal segment.

As described by Seddon in 1975 [8], there are three different classifications for peripheral nerve injuries: (1) neuropraxia which is the lowest degree of nerve injury in which the nerve remains intact but signalling ability is damaged, (2) axonotmesis which is the second class in which the axon is damaged but the surrounding connecting tissue remains intact, (3) neurotmesis or transection injuries where the nerve trunk is completely interrupted, especially those resulting in large neural gaps, may have a devastating impact on patients, quality of life, and in these cases reconstructive surgery is required as a therapeutic management to achieve nerve regeneration and function restoration. In consequence, peripheral nerve repair represents a unique challenge and opportunity to clinical and translational neurosciences [9].

2.2 Current Clinical Approaches for Treating Nerve Injuries

It is commonly accepted that physical guidance of axons is a vital component of nerve repair. In 1960s, Millesi [6] determined that the use of nerve grafts reduced tension on the damaged nerves in many cases and further enhanced functional recovery. Later research demonstrated that biochemical signals as well as physical guidance are critical for nerve regeneration [7].

For peripheral nerve injury, treatment typically consists of either direct end-to-end suture of the damaged nerve ends (Figure 2.3) or the use of an autologous nerve graft. Performing an end-to-end suture can repair small defects or gaps in the nerve. For longer nerve gaps, this surgical approach would induce tension of the suture site, inhibiting the nerve regeneration and promoting necrosis of the nerve stumps. Thus, for a larger nerve defect, an autologous nerve graft that is harvested from another site in the body is used to span the injury site. Disadvantages of this technique include loss of function at the donor

site, the need for multiple surgeries and the differences between the donor and the receptor nerve diameter, compromising the nerve regeneration [6].

For central nervous system injury, and particularly spinal cord injury, clinical treatment is less promising. Unfortunately, there is currently no treatment available to restore nerve function. After swelling from the injury subsides, patients begin a long period of rehabilitation during which time they train remaining nerves to compensate for the loss due to injury [1] [3].

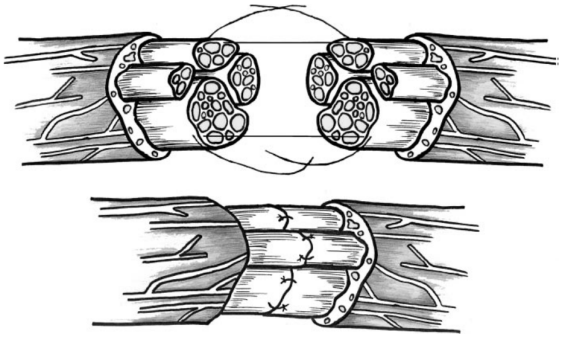

Figure 2.3. Perineural end-to-end suture of the peripheral nerve fascicles after a neurotmesis injury [6].

2.3 Challenges and Bioengineering Strategies for Nerve Repair

In the PNS, the challenge is to find an alternative to the autologous nerve graft and thus eliminate the need for two surgeries and the removal of tissue from the patient. Thus, bioengineering strategies for the PNS have focused on developing alternative treatments to the nerve graft (e.g., nerve guidance channels), especially for larger defects, and improving recovery rates and functional outcome. Many researchers are presently focusing efforts on creating physical or chemical pathways for regenerating axons [6] [7].

The CNS is a greater challenge for new therapies. The ability of spinal nerves to regenerate was not decisively shown until 1980, and it was not until after this time that research in this area rapidly developed. In addition, results from various studies have been controversial and complicated. These challenges provide fertile ground for the development of therapies and devices to enhance regeneration [6].

2.4 Neural Tissue Engineering

Nerve tissue engineering (NTE) offers great opportunities to neuroscientists and surgeons who have been collaborating to develop tissue engineered nerve grafts [9]. It is one of the most promising methods in biomedical engineering for restoring central nerve systems in humans and for repairing or replacing the function of defective or damaged tissues or organs. Nerve tissue repair is a prized treatment concept in human health care, because it has a direct impact on the quality of life [10]. Tissue engineered nerve grafts are typically composed of a physical scaffold with the introduction of support cells and/or growth factors or other biomolecular components [9].

2.5 Neural Scaffolds

The physical scaffold of tissue engineered nerve grafts, shortly called the neural scaffold, serves to: (1) direct axons sprouting from the proximal to distal nerve stump; (2) maintain adequate mechanical support for the regenerating nerve fibres; (3) provide a conduit channel for the diffusion of neurotropic and neurotrophic factors secreted by the proximal nerve stump and a conduit wall for the exchange of nutrients and waste products; (4) obviate the infiltration of fibrous scar tissue that hinders axonal regeneration; and (5) create an optimal microenvironment (niche) for nerve regeneration through the accumulation and release of exogenous and endogenous biochemical effects. For the sake of clinical use, the neural scaffold is hoped to be easy to fabricate and sterilize, and simple to implant in the body by microsurgical techniques. Up to now, a diverse array of natural or synthetic biomaterials, together with well-defined fabrication techniques, has been tried to prepare neural scaffolds that possess different structures, in which tubular nerve guidance conduit (NGC) is the basic structure [9].

2.5.1 Requirements of an Ideal Scaffold

An ideal neural scaffold has to satisfy many biological and physicochemical requirements, among which biocompatibility, biodegradability, permeability,

biomechanical properties, and surface properties are the major concerns. These required properties are mainly determined by the scaffold material and scaffold structure [9].

Figure 2.4 shows the various characteristics desired for an ideal scaffold for neural regeneration [10].

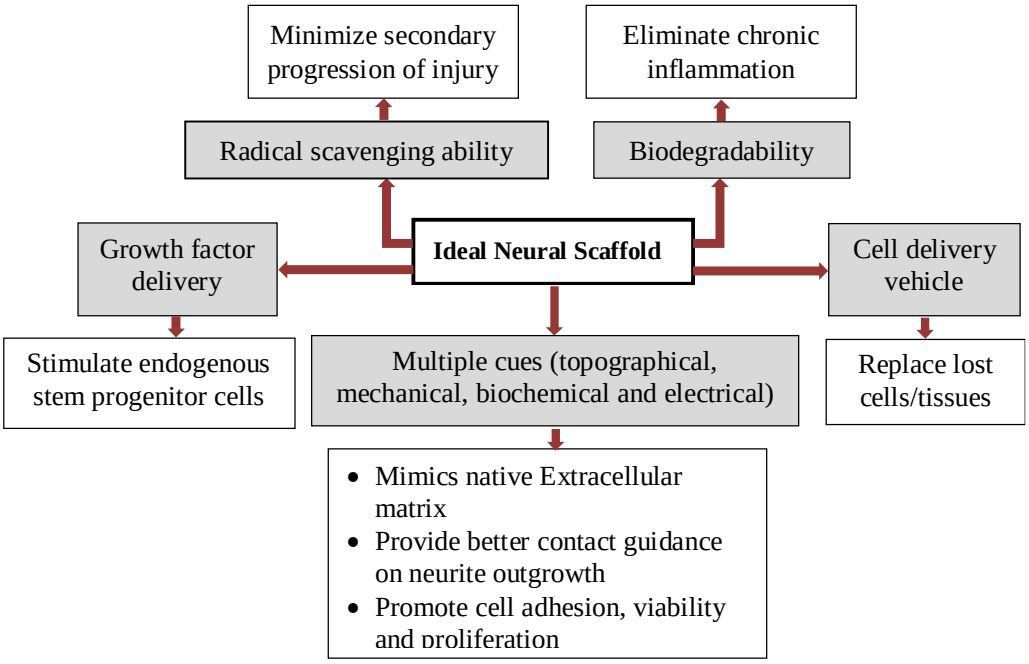

Figure 2.4. Ideal properties of a scaffold for neural regeneration [10].

2.5.1.1 Biocompatibility

The biocompatibility of neural scaffolds can be evaluated from three important aspects: (i) blood compatibility, (ii) histocompatibility, and (iii) mechanical compatibility. Blood compatibility requires that the scaffold in contact with blood does not induce hemolysis, or destroy blood components, or lead to coagulation and thrombus formation. Histocompatibility means that the scaffold has no toxic side effects on the surrounding tissues, especially neither teratogenicity nor gene mutation, while the surrounding tissues, in turn, do not induce corrosive effects or immune rejection on the scaffold. Mechanical

compatibility focuses on the matching of mechanical properties between the scaffold and nerve tissues [9].

2.5.1.2 Biodegradability

In addition to biocompatibility, an ideal scaffold has to possess a controllable ability to degrade *in vivo*. The tuneable degradation kinetics should match the rate of nerve regeneration. The ideal neural scaffold should remain intact for the time axons need to regenerate across the nerve gap and then degrade gradually with minimal swelling and foreign body reaction [9].

2.5.1.3 Permeability

As a soft tissue engineered product, a neural scaffold must have a sufficient permeability for nutrient and gas exchange, including the exchange of fluids between the regeneration environment and the surrounding tissues, avoiding the build-up of pressure due to fluid retention. Different fabrication techniques affect the permeability by altering the porous structure of neural scaffolds, and hydrophilic property of the scaffold material is another critical factor responsible for the permeability of neural scaffolds [9].

2.5.1.4 Biomechanical Properties

Sufficient mechanical strength needs to be considered when designing ideal neural scaffolds. A neural scaffold must be flexible to allow bending without kinking as well. It is important to make the right balance between the flexibility and hardness, because too stiff scaffolds are easy to cause dislocation, and too flexible scaffolds fail to support axonal regeneration [9] [11].

2.5.2 Materials Used for Neural Scaffolds

Table 2.1 provides a summary of materials in use or under investigation for nerve repair applications [6] [7].

Table 2.1.Nerve grafts and nerve conduit materials [6] [7].

Autologous tissue grafts

1. Nerve grafts (gold standard)
2. Vein grafts
3. Muscle grafts
4. Epineurial sheaths
5. Tendon graft

Nonautologous/acellular grafts

1. Immunosuppression with allografts
2. Acellular allografts and xenografts
   - Thermal decellularization
   - Radiation treatment
   - Chemical decellularization
3. Small intestinal submucosa (SIS)
4. Human amnion

Natural-based materials

1. ECM protein-based materials
   - Fibronectin
   - Laminin
   - Collagen
2. Hyaluronic acid-based materials
3. Fibrin/fibrinogen
4. Chitosan
5. Other materials (alginate, agarose, etc.)

Synthetic materials

1. Biodegradable synthetic materials
   - Poly(lactic acid) (PLA)
   - Poly(lactic-co-glycolic acid) PLGA
   - Poly(caprolactone)
   - Poly(organo)phosphazene
   - Poly(3-hydroxybutyrate)
   - Poly(ethylene glycol) “glue”
   - Biodegradable glass
2. Electrically active materials
   - Piezoelectric
   - Electrically conducting
3. Nonbiodegradable synthetic materials
   - Silicone
   - Gore-Tex or ePTFE

2.5.2.1 Natural Polymers

The selection of biomaterials is very important for the fabrication of neural scaffolds. A wide variety of biomaterials has been attempted, which are of either natural or synthetic origin. Natural polymers, such as chitosan, alginate, and especially collagen and fibrin, due to their structural similarity with the neural structure, and properties such as cell attachment, growth and proliferation, have more advantages than synthetic polymers, but their low mechanical properties and their tendency to swell is still a problem to overcome to foster the widespread use of such materials. However, designs with small nerve gaps have been responsive [12] [13]. Biodegradable nerve guides must be preferred since no foreign body material will be left in the host after the device has fulfilled its task [12].

2.5.2.1.1 Collagen and Other ECM Components

Collagen is the major component of the extracellular matrix and is known to promote cellular proliferation and tissue healing. Among the most promising biomimetic biomaterials for nerve regeneration, collagen proved to lead to functional recovery similar to nerve autografts in experimental animal models. Conduits derived from biologic molecules like collagen have demonstrated improved regeneration [14] [15]. Gelatin, derived from denatured collagen, is also the first biodegradable material examined for preparing neural scaffolds. Other ECM molecule-derived materials, for example, laminin and fibronectin, are also used for the fabrication of neural scaffolds [9].

2.5.2.1.2 Alginate

Alginate, commonly purified from seaweed, is a naturally occurring copolymer [9]. Prang *et al.* [16] have assessed the capacity of alginate gels to promote directed axonal regrowth in the injured mammalian central nervous system. The alginate scaffolds also promoted adult peripheral nerve survival and highly oriented axon regeneration. This was the first instance of using alginates to produce anisotropic-structured capillary gels, so

further studies are needed to investigate the long-term physical stability of the alginate scaffolds, because central nervous system axon regeneration can take many months to occur.

2.5.2.1.3 Polysialic Acid

Polysialic acid (PSA) is a relatively new biocompatible and bioresorbable material for artificial nerve conduit. PSA shows stability under cell culture conditions and allows for degradation induced by enzymes. It has also been discovered recently that PSA is involved in steering processes like neuritogenesis axonal path finding, and neuroblast migration. Animals (adult female Sprague–Dawley rats) with PSA genetically knocked out express a lethal phenotype which has unsuccessful path finding, ie, the nerves connecting the two brain hemispheres are aberrant or missing. Thus, PSA is vital for proper nervous system development [12].

2.5.2.1.4 Chitin and Chitosan

Chitin is the second most abundant polysaccharide found in nature next to cellulose, and can be isolated from the outer shell of crustaceans, insect exoskeletons, and fungal cell walls. Chitin is extensively applied in a wide range of biomedical fields [9]. Chitins and modified chitins exert a number of beneficial actions, such as: (1) they stimulate macrophages by interacting with receptors on the macrophage surface (2) they stimulate macrophages to produce cytokines and other compounds that confer nonspecific host resistance against bacterial and viral infections, and antitumor activity [17]. The ideal structure of chitin is a linear polysaccharide of β (1→4)-2-acetamido-2-deoxy-D-glucopyranose, where all residues are comprised entirely of N-acetyl-glucosamine residues are fully acetylated. The ideal structure of chitosan, the principal derivative of chitin, is a linear polymer of β (1→4)-2-amino-2-deoxy-D-glucopyranose, where all residues are comprised entirely of N-glucosamine residues or are fully deacetylated. Figure 2.5 is showing the ideal chemical representation of chitin and chitosan [18].

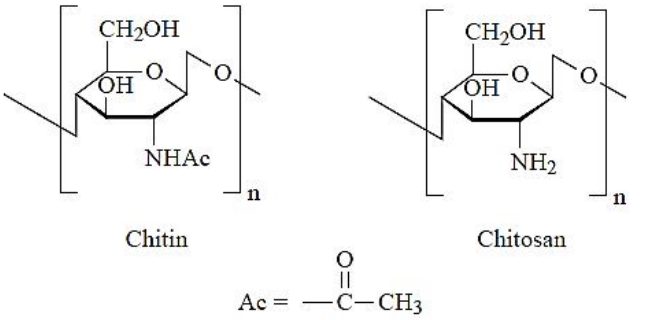

Figure 2.5. Ideal chemical representation of chitin and chitosan [18].

However, the traditional sources of chitin and chitosan are not in fact 100% acetylated or deacetylated. They exist as a co-polymer of N-acetylglucosamine and glucosamine, as represented in Figure 2.6. The difference between chitin and chitosan is their acetyl content. Chitin is made up of more than 50% (more commonly 70-90%) acetamido groups while chitosan commonly having 70-90% amino groups. The main parameters influencing the chemical characteristics of chitosan are its degree of acetylation that could be within the range of 30-95%, and molecular weight, which can vary from 300 to over 1000 kDa [18] [19] [20].

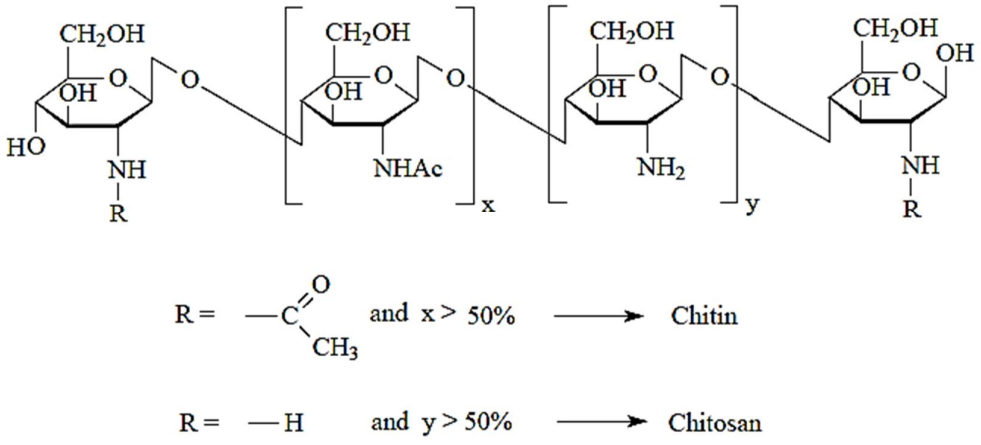

Figure 2.6. Chemical structural representation of chitin and chitosan illustrating the copolymer character of the biopolymers [18].

Chitosan is highly bioactive, biodegradable and biocompatible; so, it is widely used in biomedical applications, such as skin substitutes, wound healing, nerve regeneration, gene delivery, cartilage and bone tissue regeneration [18]. Chitosan has quite positive effects on the nerve regeneration. It has been showed that when chitosan is used, it facilitates nerve healing and improves the nerve differentiation and growth. It also shows antifungal, antitumoral, anticholesteremic, antibacterial and antimicrobial characteristics because the cationic moieties of chitosan molecules can interact with anionic cell wall of bacteria/micro-organisms and rupture their cell wall that reduces the bacteria attachment and survivability [20] [21] [22].

Chitosan is insoluble in neutral or basic pH solutions, but soluble in acidic solutions (< pH 6.5), because of presence of primary amine groups which make chitosan a cationic polyelectrolyte (pKa ~ 6.5) and allow it to be coupled covalently to the various biomolecules, along with its other primary and secondary hydroxyl functional groups [21] [23].

2.5.2.2 Synthetic Polymers

In addition to naturally derived biopolymers, synthetic polymers constitute another class of promising biomaterials for fabricating neural scaffolds due to their tuneable chemical and physical properties [9].

Synthetic materials are attractive because their chemical and physical properties (e.g., degradation rate, porosity, mechanical strength) can be specifically optimized for a particular application [7] [12]. In some cases, synthetic biomaterials are cheaper than natural ones, can be produced in larger quantities with uniform properties and have longer shelf life [11]. However, the biocompatibility of synthetic materials poses a challenge because the body's inflammatory response can vary considerably from one material to another. In addition, some synthetic materials that are tolerated by the body's immune system are unfortunately incompatible with cell adhesion and tissue repair. These materials are often modified to render them more "cell friendly" [7] [12].

To select an appropriate synthetic material, there are several general properties that all nerve guidance channels should possess: (1) they must be readily formed into a conduit with desired dimensions, (2) they must be sterilizable, (3) they must be tear resistant, and (4) they must be easy to handle and suture. Permanent materials pose a higher risk for infection, are more likely to provoke a chronic inflammatory response, and have the potential to compress the nerve over time. Thus, a nerve guide that degrades as the nerve regenerates is preferred. Additionally, guidance channels should be pliable, but should maintain their shape and resist collapse during implantation and over the time course for regeneration. Research has also shown that guidance channels should be semipermeable and should have a smooth inner wall. Properties of the ideal nerve guidance channel are shown in Figure 2.7 [7] [12].

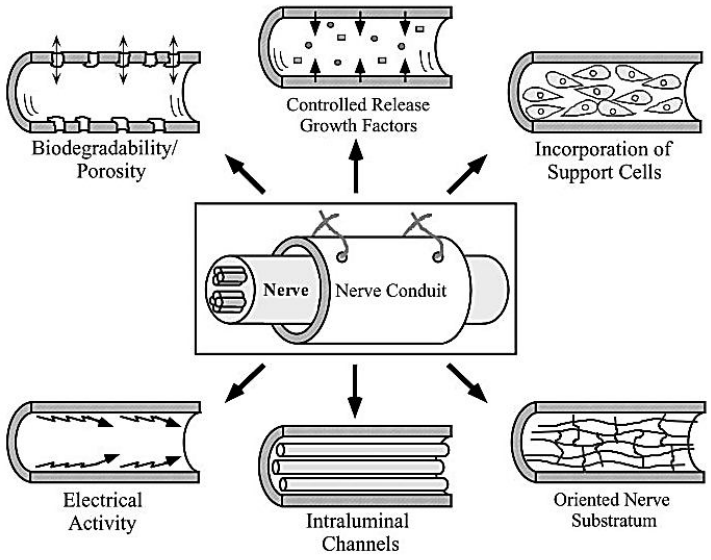

Figure 2.7. Properties of the ideal nerve guidance channel [7].

So the factors that control material selection include biocompatibility, biodegradability, mechanical integrity and controllability during nerve growth, implantation and sterilization [12].

2.5.2.2.1 Non-absorbable Synthetic Polymers

Beginning in the early 1980s, replacement surgery using artificial nerve conduits made from non-absorbable materials, such as silicone Figure 2.8), has been in use for the treatment of severed nerves. All these reports, however, are of studies demonstrating recovery in morphologic continuity of a nerve with an extremely small gap of about 10 mm in small laboratory animals, and recovery of motor function has rarely been achieved. The outcome is in no way superior to that of nerve autografting in any of the reported studies. Elastomer hydrogels or porous stainless steel has also been used for nerve regeneration. However, these artificial materials have the disadvantages of engendering chronic foreign body reaction due to scar tissue formation, inflexibility, and lack of stability [12] [14].

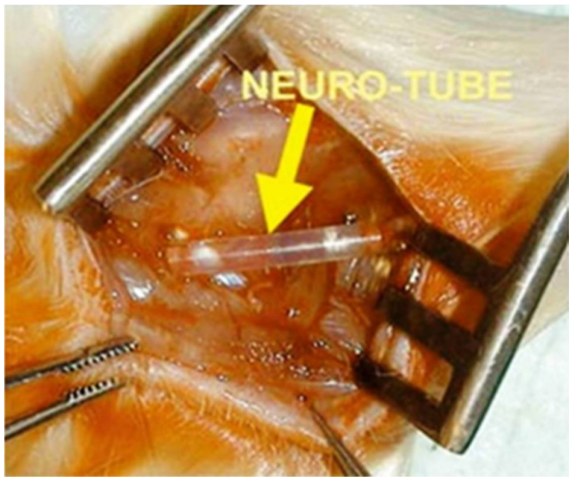

Figure 2.8. Silicone tube for nerve regeneration after a neurotmesis injury [12].

2.5.2.2.2 Absorbable Synthetic Polymers

It became recognized from the latter half of the 1980s onwards that degradable-absorbable materials are preferable in the body after attaining nerve regeneration. With the progress in material synthesis and bridging techniques, artificial nerve guides made of absorbable synthetic materials, have been developed. Substances such as polyglycolic acid (PGA) and polylactic acid (PLA) or polyhydroxybutyrate are under investigation as biodegradable-absorbable synthetic materials for nerve regeneration [12] [14]. Khorasani *et al.* [24] have designed PLLA tubes for nerve regeneration and studied cellular investigations and *in vitro* assessments. These polymers are brittle, and they do not have regions permissible for chemical modification. In addition, they degrade by bulk rather than by surface, which is not a smooth and ideal degradation process. In an attempt to overcome the lack of functionality, free amines have been incorporated into their structures from which peptides can be tethered to control cell attachment and behaviour. Other biodegradable poly(esters), such as poly(caprolactones), have also demonstrated promise for nerve regeneration applications. In addition to poly(esters), biodegradable poly (urethane), poly(organo phosphazene), methacrylate-based hydrogels, and poly(3-hydroxybutyrate) have shown a capacity for guiding regeneration. Biodegradable glass tubes have also been studied, but results of pre-clinical studies have not been optimistic [12] [14].

2.5.2.3 Composite Nerve Guides

Composite scaffold materials can be designed from both synthetic and natural polymers embedding particles of bioactive and biodegradable inorganic components such as calcium phosphates or bioglasses.

Clinically, type I collagen conduits [25], chitosan [26] [27] [28] and polyphosphoesters such as poly (DL-lactide–caprolactone) [29] [30] are popular resorbable biomaterials used in nerve tissue repair. However, there is significant scope for improvement with these materials.

In addition to materials which can interact with the body to improve regeneration, it is required to make a balance among mechanical properties, biocompatibility, and controlled degradability. Accordingly, composite materials offer significant opportunities for investigation [31]. Composites that have combined biodegradable polymers and bioactive inorganic phases such as hydroxyapatite (HA) [32] [33], β-TCP [34] [35] or bioactive glass [36] [37] [38] have resulted in resorbable scaffolds with tailored biocompatibility and improved physical and mechanical properties, especially in hard tissue regeneration. Additionally, some of degradation by-products can be clinically beneficial. So, composite materials, if properly designed and optimized, may allow the development of scaffolds with tailored physical, biological and mechanical properties to suitably match the application of peripheral nerve repair [31].

Guidance of developing axons involves turning of the motile tip, the growth cone [39], and is dependent on extracellular cues, including ionic messengers. Divalent calcium ion (Ca^{2+}) is the most widely used messenger which regulates turning (guidance) and extension of the growth cone [40] [41]. Zinc (Zn^{2+}) is the second most existing trace element in the human body and is required for normal growth and correct immune function [42], it is also an effective antibacterial agent [43]. It has also been suggested that Zn^{2+} may be a valuable specific therapy for uremic polyneuropathy and nerve development [42]. From a material viewpoint, the synthesis of degradable bioglasses containing these elements is a possible way to release controlled levels of these therapeutic ions in controlled levels is possible via the synthesis of degradable bioglasses containing these elements [44] [[45]. Therefore, combining such bioglasses with polymers appears as a quite promising strategy to enhance the mechanical properties of the scaffolds and their biological responses *in vivo*.

Bioactive materials elicit an appropriate biological response when implanted *in vivo*, enabling the formation of bonds between materials and surrounding tissues. Bioactive glasses are commonly described as ideal materials for bone tissue regeneration due to their ability to promote osteointegration, mesenchymal stem cell differentiation, and promotion of growth factor [46]. Bioactive glasses have been used in biological applications since Hench described their use the early 70s. There have been interesting research works about bioactive glasses in science and biomedical applications over the last two decades, as evidenced by the growing number of publications in this field [47]. Bioactive glasses have shown tailored therapeutic ion release, primarily in hard tissues. However, as described

before, controlled degradation and release of therapeutic ions from these biomaterials may also play an important role in soft tissue regeneration such as repairing of peripheral nerve gaps [44]. There has been relatively little research on the application of bioactive glasses on repairing of peripheral nerve gaps. According to Buting *et al.* [36], fibres of Bioglass® 45S5 can form a biocompatible scaffold to guide re-growing peripheral axons in vivo. Kehoe [31] has successfully designed a nerve guidance conduit consists of PLGA (lactic to glycolic acid mole ratio, 75:25) and a zinc-silicate based bioactive glass and evaluated the cytotoxicity and mechanical properties of conduit. Zhang *et al.* [44] have designed silica-based glasses (Si–Na–Ca–Zn–Ce system) and investigated composition-structure-property relationships in these systems with respect to their potential use as fillers in polymeric (PLGA) composite constructs for peripheral nerve regeneration. They have evaluated the Ca^{2+} and Zn^{2+} release profile for this purpose. Release of such elements, at appropriate levels, from peripheral nerve guidance conduits may be advantageous with respect to the repair of peripheral nerve discontinuities.

Goel *et al.* [45] have designed and developed alkali-free series of bioactive glasses in the glass system $CaO–MgO–SiO_2–P_2O_5–CaF_2$ along the diopside ($CaMgSi_2O_6$)–fluorapatite ($Ca_5(PO_4)_3F$)–TCP ($3CaO.P_2O_5$) join. FastOs®BG is a common designation for these developed bioactive glasses, which can be doped with some other elements such as Sr, Zn, Mn, etc. It was demonstrated that these glasses exhibit high rate of *in vitro* bioactivity, but detailed *in vitro* cell culture and *in vivo* tests need to be carried out on this bioactive glass in order to prove their efficacy for application in human biomedicine. On the other hand, the bioactive glasses having high alkali metal content (sodium and potassium) are sensitive to water uptake resulting in swelling and cracking of the polymer matrix embedding them in composites [48]. So, it can be concluded that by using these alkali-free bioactive glasses embedded in polymer matrix, the rate of swelling and degradation of composites can be controlled which is important in nerve tissue regeneration. In fact, the resistance to deformation determines whether the conduit can be used *in vivo* due to the various stresses from the surrounding tissue while the resistance to swelling protects the regenerated nerve axons from being compressed by the conduit wall. The swelling should be moderate [49] [50].

Recently, chitosan-based nerve conduits extensively developed to bridge large peripheral nerve gaps have achieved considerable success [50] [51] [52] [53] [54].

However, there is currently no research using the combination of chitosan and FastOs®BG in nerve tissue repair. Thus, in this study, novel biodegradable composite membranes based on chitosan and FastOs®BG doped with 4 mol% Zn (FastOs®BG-Z4) were synthesized aiming at nerve regeneration applications. It is hypothesized that FastOs®BG-Z4 particles will improve the mechanical properties of the membranes to resist muscular contractions and maintain a stable support structure to provide space for nerve regeneration. It is also expected that the controlled ionic release from FastOs®BG-Z4 will assist in nerve regeneration and in preventing oxidative stress [45].

2.6 Cross-linked Chitosan Scaffolds

For generating chitosan scaffolds, the polymer has to be cross-linked to raise its stability. Cross-linking treatments are split into two groups: chemical cross-linking and biophysical cross-linking. Chemical methods include the use of various chemical reagents, whereas biophysical methods include the use of UV light and dehydrothermal cross-linking [2].

Chitosan can be cross-linked either ionically or covalently. As ionic cross-linkers, polyanions like triphosphate, citrate or natural polymers like hyaluronic acid or chondroitin sulphate are used. In this connection the polyanion can interact with chitosan via electrostatic forces to form an ionic cross-linked network. The other possibility is a covalently formed network with the amino and hydroxy-groups of chitosan reacting with functional groups of cross-linker molecules. Covalently cross-linked networks can be formed by genipin, di- or polyaldehydes (glutaraldehyde, oxidised starch and oxidised cylcodextrin). Also, carboxylic acids, azides, epoxides, diisocyanates and silanes are compounds that have been used as covalent cross-linkers [55] [56].

2.6.1 Glutaraldehyde

Glutaraldehyde (GT) is one of the most popular cross-linking treatments for biological tissues. It is a bifunctional cross-linker, which reacts with chitosan via either a Schiff base

reaction, leading to imine functionality (Figure 2.9), and/or through Michael-type adducts with terminal aldehydes, leading to the formation of carbonyl groups. Although being widely used, GT mediated cross-linking is often cited as being undesirable as it introduces cytotoxic aldehyde molecules [57] [58].

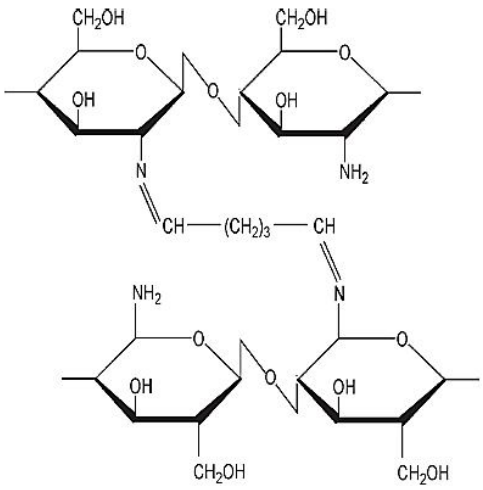

Figure 2.9. The chemical structure of GT-cross-linked chitosan [57].

2.6.2 Genipin

Genipin (GP) (Figure 2.10) can be obtained from its parent compound, geniposide, which is isolated from the fruits of Gardenia jasminoides ELLIS. GP and its related iridoid glucosides have been widely used as antiphlogistics and cholagogues in herbal medicine. It has been used as a cross-linking agent for the fixation of biological tissues as bioprostheses. It can react spontaneously with amino acids or proteins to form dark blue pigments. GP is about 5000–10,000 times less cytotoxic than glutaraldehyde [59] [60] [61].

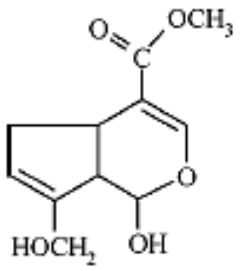

Figure 2.10. Schematic of GP chemical structure [60].

Mi *et al.* [62] have shown that cross-linking of chitosan membrane using GP reduced its tensile strain, swelling ratio and enzymatic degradability. According to Chiono *et al.* [63], chitosan/gelatin blends cross-linked with optimal additions of GP were able to support neuroblastoma cell adhesion and proliferation, and cross-linking degree increased with increasing the GP amount as a result of higher water stability and mechanical stiffness. Sung [64] has shown that differences in cross-linking structure may affect the mechanical properties and the bonding characteristics of the graphs to living tissues.

2.7 Fabrication Techniques for Nerve Guidance Conduit

To more accurately mimic natural repair in the body, recent studies have focused on the use of various advanced approaches to create complex guidance channels and to combine multiple stimuli into a single therapy. With regard to advanced guidance channel fabrication, most techniques have focused on creating intricate internal structures that more accurately mimic the nerve architecture, such as the inclusion of fibres and channels to guide individual nerve fibres. In general, researchers have attempted to improve the neural scaffold properties by several novel fabricating techniques such as magnetic polymer fibre alignment, injection moulding, solid free-form fabrication, ink-jet polymer printing, nanofibre self-assembly, solvent casting and particulate leaching, gas foaming, emulsification/freeze-drying, liquid-liquid phase separation, electrospinning, incorporating nerve growth factors in the scaffold and improving the wettability of the scaffold surface by surface modifications [10] [14]. Each technique is briefly described below.

2.7.1 Magnet Alignment and Injection Moulding

Nerve guidance channels have been predominantly fabricated as hollow tubes or as porous foam rods because of the ease in manufacturing these devices. For hollow tubes, it is known that the body normally generates an oriented fibrin matrix after placement of a hollow conduit across a nerve defect, which serves as a critical precursor to axonal regeneration. With regard to foam rods, it is questionable whether an amorphous irregular structure optimally guides axonal regeneration. Thus, to mimic natural repair in the body and to shorten the time required for regeneration, more recent studies have focused on the modification of nerve guidance channels with internal matrices of longitudinally aligned fibres or channels. These devices often require more advanced processing techniques. As a means to provide the necessary matrix alignment and also improve upon processing conditions, magnetic fields have been used to orient protein polymers. In a different approach, a novel foam-processing technique, utilizing low-pressure injection moulding, created highly porous conduits from PLGA with continuous longitudinal channels [10].

2.7.2 Phase Separation

When using phase separation, a porous structure can be easily obtained by adjusting thermodynamic and kinetic parameters. However, because of the complexity of the processing variables involved in the phase separation technique, the pore structure cannot be easily controlled. Moreover, it is difficult to obtain large pores, which may exhibit a lack of interconnectivity [65].

2.7.3 Gas Foaming

Gas foaming has the advantage of room temperature processing but produces a largely nonporous outer skin layer and a mixture of open and closed pores within the centre, leaving incomplete interconnectivity. The main disadvantages of the gas foaming is that it often results in a non-connected cellular structure within the scaffold [66].

2.7.4 Solvent Casting

Solvent casting is a combination with particulate leaching method, which involves the casting of a mixture of monomers and initiator solution and a porogen in a mould, termed polymerization, followed by leaching-out of the porogen with the proper solvent to generate the pores. It is inexpensive but still has to overcome some disadvantages in order to find engineering applications as structures that facilitate either tissue regeneration or repair during reconstructive operations [66].

2.7.5 Freeze Drying

Freeze drying technique is based upon the principle of sublimation to fabricate porous scaffolds. The typical process would be to dissolve the polymer into a solvent in order to form a solution of desired concentration. Then the solution is frozen and solvent will be removed by lyophilisation under a high vacuum. In this method, the pore size and porous structure can be controlled by the freezing rate, pH, and temperature. However, the small pore size formed in this technique is a concern for some applications and also the time consuming lyophilisation step [1].

Generally, the freeze-drying process can be split into two parts: freezing and drying. During freezing the temperature of the solution is lowered and a phase change occurs, where liquid water is converted into ice crystals. The cooling rate is an important aspect of the freezing cycle because it affects the ice crystal formation during freezing. Fast rates of cooling have a tendency to produce many small ice crystals. These crystals may not be continuous, but they are generally homogeneously distributed throughout the frozen solution. A slow rate of freezing will result in a more connected ice crystal structure with larger crystals [2].

So, to produce large ice crystals, the freezing temperature should be as high as possible and the time for crystallization should be extended. To produce smaller crystals, freezing should take place under low temperature conditions and the freezing rate should be high in order to reduce the time available for ice crystals to grow [67].

The next step in the process is drying in which heat is added to the material under a vacuum. Under these conditions the ice crystals are sublimated from the solute. The sublimated water vapour is then trapped on a condenser, and the process is complete [2].

With freeze drying system, two kinds of biomaterials with different properties can be combined to produce scaffold structures with good biocompatibility in the inner layer and with the desired mechanical strength protruded by the outer layer. The forming precision is high, the wall thickness can be controlled, and a tight connection between the two layers can be achieved [66].

Both homogeneous aqueous solutions and heterogeneous dispersions can be frozen and freeze-dried to prepare materials with relatively disordered macroporous structures. Alternatively, the freezing process can be performed in a more controlled manner to orientate the growth of the ice crystals in one direction. Zhang *et al.* [67] have described developments in the use of directional freezing techniques to produce porous materials where the orientation of the crystal growth defines the pore structure. They outline how these methods can produce complex composite materials with a range of aligned pore architectures. Figure 2.11 shows a schematic diagram of the directional freezing process. Ice crystals grow from the bottom [67].

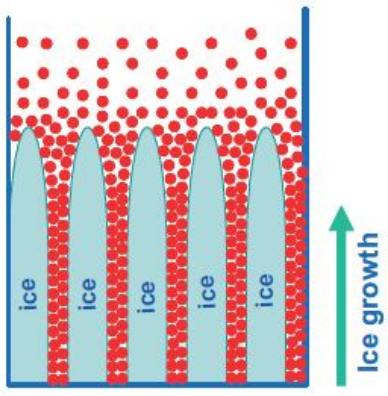

Figure 2.11. Scheme showing the directional freezing process [67].

Particles and polymeric molecules are excluded from the ice and aggregate between the growing ice crystals. After the freezing is complete, removal of the orientated ice by freeze drying leads to the formation of aligned structures.

2.7.6 Electrospinning

Electrospinning is a simple, unique, and efficient method which has the possibility of producing ultrafine multicomposite fibres with spatial orientation and nanodimensions with high surface area and controlled pore geometry [68]. A polymer solution or melt is drawn from a nozzle by applying a force of gravity or mechanical pressure combined with an electric field of high voltage (10–20 kV). When the electric charge overcomes the surface tension of the polymer solution droplet, a polymer jet is sprouted, followed by solvent evapouration which forms the solid nanofibres [69]. The properties of the electrospun fibres such as the diameter, orientation, and porosity influence cell adhesion, proliferation and processes such as the transportation of nutrients (e.g. metabolites, oxygen) to and from the cells. The orientation of fibres within the engineered scaffold play an important role in mimicking the extracellular matrix (ECM) because many tissues in the body (e.g., endothelial and nerve cells) have regular oriented architecture, which is strongly correlated to their distinguished mechanical properties and particular functions. These described factors should be considered while designing and fabricating engineered scaffolds for nerve tissue engineering [68].

2.7.7 Solid Freeform Fabrication

Recently, the emergence of advanced techniques for polymer processing such as solid freeform fabrication (SFF) has gained tremendous attention in the bioengineering field because of its ability to design of intricate devices for peripheral nerve and spinal cord repair. SFF can fabricate 3D porous scaffolds with high degree control microstructure directly from a computer model. Some limitations do exist, including the high cost of the instrument and the inability to incorporate biological components under some processing conditions [6] [70].

Different techniques for the tissue engineering scaffolds fabrication are summarized and compared in Table 2.1 [1] [71].

Table 2.1. Comparison of different techniques used for the fabrication of scaffolds for tissue engineering applications [1] [72].

Methods	Pore size (µm)	Porosity (%)	Advantages	Disadvantages
Solvent Casting/Particulate Leaching	30-300	20-50	Controlled porosity, pore size, inexpensive	Limited thickness, lack of mechanical strength, harmful organic solvent and porogens residue
Phase Separation	-	-	Ease to combine with other techniques, ability to keep the activity of biomolecules	Difficulty to precisely control scaffold morphology
Freeze Drying	<200	<97	Simplicity of utilization, no high temperature or leaching, highly porous structures, high interconnectivity	Small pore size and long processing time
Electrospinning	-	-	Controllable porosity, pore size, and fibre diameter	Limited mechanical properties, decreased pore size with increasing thickness
Rapid Prototyping	40-150	<90	Excellent controlled geometry, porosity, good repeatability	Expensive equipment, limited polymer type

Chapter 3

Experiments

3.1 Materials

An alkali-free bioactive glass was selected from a series of compositions (mol%): 36.07 CaO – (19.24 – *x*) MgO – *x*ZnO 5.61 P_2O_5 – 38.49 SiO_2 – 0.59 CaF_2 [45], where *x* was fixed at 4.00 mol% (FastOs®BG-Z4). The synthesis included high-purity powders of SiO_2 (purity >99.5%), $CaCO_3$ (>99.5%), $MgCO_3$ (BDH Chemicals Ltd., UK, purity >99.0%), ZnO (Sigma Aldrich, Germany, 99.9+%), $NH_4H_2PO_4$ (Sigma Aldrich, Germany, >99.0%) and CaF_2 (Sigma Aldrich, Germany, 325 mesh,>99.9%), as described elsewhere [45]. A homogeneous batch (~100 g) obtained by ball milling, was preheated at 900ºC for 1 h for decarbonisation and then melted in a Pt crucible at 1550ºC for 1 h in air. The molten glass was poured in cold water to obtain a frit, which was then dried and milled in a high-speed agate mill, resulting in fine glass powders with mean particle sizes of ~10–20 μm (determined by light scattering technique; Coulter LS 230, Beckman Coulter, Fullerton, CA; Fraunhofer optical model). The amorphous nature of glasses was confirmed by X-ray diffraction (XRD) analysis (Rigaku Geigerflex D/Max, Tokyo, Japan; C Series; Cu K_α radiation; 2θ angle range 10 – 80; step 0.02 s^{-1}).

Commercial chitosan with medium molecular weight and a deacetylation percentage (DD) of ~85% was purchased from Sigma-Aldrich (Germany) and lactic acid (LA) was purchased from Fluka (Germany). Glutaraldehyde (50%) was a product of USA and genipin was obtained from Challenge Bioproducts (Taiwan). Distilled water was used to prepare all the solutions.

3.2 Preparation of Chitosan/FastOs®BG-Z4 Membranes

The chitosan/FastOs®BG-Z4 composites were prepared as schematized in Figure 3.1. A 1 vol.% lactic acid (LA) solution was firstly prepared in distilled water. Then, a 2 wt.% chitosan was added to this 1 vol.% LA solution, which was kept under magnetic stirring overnight at 50ºC. The as obtained chitosan solution was filtered through a 150 μm sieve and FastOs®BG-Z4 powder was then added in order to have a chitosan:Fastos®BG-Z4 weight ratio of 50:50. Different amounts of genipin and glutaraldehyde (0.01, 0.05 and 0.5 wt.% relative to the dry mass of chitosan) were separately added as cross-liking agents for

chitosan matrix. The as obtained composite systems were poured into closed special moulds to avoid evapouration and left for 20 minutes in an oven at 60ºC to promote reticulation. The prepared gels were frozen at –20ºC for 24 h and –80ºC for 4 h to evaluate the effect of freezing temperature on the membrane properties. The frozen samples were then lyophilized in a freeze-dryer (Labconco, USA) (Figure 3.2) at –50ºC, under vacuum (45×10^{-3} mbar), for 72 h to obtain porous membranes. Dried membranes were stored in a desiccator at room temperature until use.

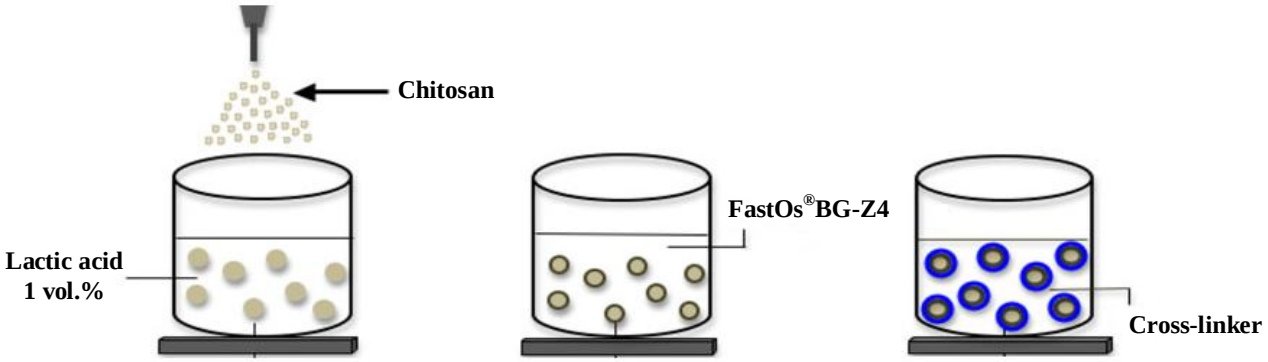

Figure 3.1. Schematics of the composite chitosan/FastOs®BG-Z4 membranes preparation process.

Figure 3.2. The freeze dryer system (Labconco, USA) used for lyophilization of chitosan-based membranes.

The 50:50 weight ratio composite chitosan:FastOs®BG-Z4 membranes containing 0.00, 0.01, 0.05 and 0.50 wt.% of genipin (GP) and glutaraldehyde (GT), frozen at –20ºC and –80ºC, were labelled as shown in Table 3.1.

Table 3.1. Codes of composite chitosan/FastOs®BG-Z4 membranes cross-linked with GP and GT frozen at –20ºC and –80ºC.

Chitosan:FastOs®BG ratio	Genipin (wt.%)	–20ºC	–80ºC
50:50	0.00	GP00-20	GP00-80
	0.01	GP01-20	GP01-80
	0.05	GP05-20	GP05-80
	0.50	GP50-20	GP50-80

Chitosan:FastOs®BG ratio	Glutaraldehyde (wt.%)	–20ºC	–80ºC
50:50	0.00	GT00-20	GT00-80
	0.01	GT01-20	GT01-80
	0.05	GT05-20	GT05-80
	0.50	GT50-20	GT50-80

3.3 Characterization and Properties Evaluation

3.3.1 Rheological Properties

The effects of adding different amounts of GP or GT (Table 3.1) or FastOs®BG-Z4 powder alone, and concomitantly with the different amounts cross-liking agents on the gelation behaviour of the final mixtures were evaluated under oscillatory tests carried out in a C-VOR rheometer (Bohlin Instruments, USA) (Figure 3.3) equipped with cone and plate geometry (Ø = 20 mm, angle =1º, gap = 150 µm) at 60ºC. To minimize the effect of the water evaporation, a "solvent trap" was used, in order to saturate the surrounding sample environment with water. The oscillatory rheological parameters used to compare

the viscoelastic properties for all the systems were the storage modulus (G′) and the loss modulus (G″).

Preliminary tests were run to determine the linear viscoelastic range in which the oscillatory tests would be performed, i.e. the range where response of the sample is within the linear viscoelastic region.

Temperature sweep measurements were also performed for all the systems in order to determine the required temperature-time schedule for reticulation to help stipulating the experimental conditions to be used in further experiments. Gelation experiments were then conducted at a constant frequency (1 Hz) and stress (5 Pa) by recording the variation of the elastic modulus (G′) and viscous modulus (G″) along the time at a constant temperature of 60ºC. The gelation time for each system was considered to be the corresponding to the respective crossover point of G′ and G″.

Figure 3.3. The C-VOR rheometer (Bohlin Instruments, USA) used in this study.

3.3.2 FTIR-ATR Spectroscopy Analysis

Fourier transform infrared spectroscopy-Attenuated total reflectance (FTIR Bruker Tensor 27) was used to investigate the characteristic functional groups. For this purpose, 3 samples GP00 (GT00), GP05-20, and GT05-20 (Table 3.1) were selected and tested within the wavelength range 300 – 4000 cm^{-1}, using 276 scans and 4 cm^{-1} resolution.

3.3.3 Microstructure Analysis

The morphology of the chitosan/FastOs®BG-Z4 scaffolds' cross-sections were observed by scanning electron microscopy (SEM, Hitachi, S-4100, Tokyo, Japan, 15-kV acceleration voltage). The samples were cut into 5 mm diameter discs and coated with a thin layer of a gold-palladium alloy by using sputter coater (Polaron Equipment Limited SEM coating unit E5000) before SEM analysis.

3.3.4 Cross-linking Degree Determination

The cross-linking degrees of scaffolds reticulated with GP and GT were determined by the ninhydrin (NHN) assay described elsewhere [72] [73]. The NHN solution was prepared as follows:

Solution A:

25 ml distilled H_2O containing 1.05 g citric acid (99%), 0.4 g NaOH (≥97%) and 0.04 g $SnCl_2.2H_2O$ (98%);

Solution B:

25 ml ethylene glycol monomethyl (≥99.5%) containing 1 g NHN.

The two solutions were mixed with stirring for 45 min and the final NHN solution was stored in a dark bottle.

Before determination of cross-linking degree, 4 mg of the lyophilized scaffolds from each group was heated with 2 ml NHN solution to 100ºC in a water bath for 20 min. The solution was then cooled down to 20ºC, diluted with 5 ml of 50% isopropanol, and the optical absorbance of the solution at 570 nm was recorded with a spectrophotometer (UV-210, Hitachi, Japan) (Figure 3.4) using glycine at various known concentrations (1.0, 2.0, 3.0, 4.0, and 5.0 mg/ml) as standard.

It is known that, after heating with NHN, the amount of free amino groups in the test sample is proportional to the optical absorbance of the solution. The measured concentration was divided by the sample weight and multiplied by the sample molecular weight to obtain the mole NH_2/mole sample. The extent of cross-linking (*%CL*) for each sample was calculated using the following equation:

$$\%\boldsymbol{CL} = \frac{(\boldsymbol{NHN\ reactive\ amine})_{\boldsymbol{control}} - (\boldsymbol{NHN\ reactive\ amine})_{\boldsymbol{fixed}}}{(\boldsymbol{NHNreactive\ amine})_{\boldsymbol{control}}} \times \mathbf{100}$$

where 'control' is the mole fraction of free NH_2 in non-cross-linked sample (chitosan/FastOs®BG-Z4 without GP or GT) and 'fixed' is the mole fraction of free NH_2 remaining in cross-linked sample. Each determination was performed in triplicate (n = 3).

Figure 3.4. The spectrophotometer (UV-210, Hitachi, Japan) used in this study.

3.3.5 Pore Size and Porosity Measurement

The porosity of the chitosan scaffolds was evaluated using cylindrical samples of 2.4 cm (diameter) × 0.9 cm (height) with the ethanol replacement method described by Yang *et al*. [74]. Porosity (%) was calculated by the following equation:

$$Porosity\ (\%) = \frac{V_p}{V_t} \times 100 = \frac{m_{24} - m_0}{V_t \times \rho} \times 100$$

where V_t is the total volume of the chitosan scaffold (cm^3), V_p is the pore volume of the chitosan scaffold (cm^3), m_{24} is the weight (g) of the chitosan scaffold after incubation with ethanol for 24 h, m_0 is the original weight (g) of the chitosan scaffold, and ρ is the density of ethanol (0.789 g cm^{-3}).

Equivalent circle diameter (ECD) of the pores was calculated by using ImageJ software. In brief, the pores were manually picked by built-in drawing functions, and the area (A) of

each pore was subsequently measured by using 'Measure' function. The pore diameter was then calculated according to following formula:

$$D = \sqrt{4A/\pi}$$

To validate this measurement statistically, at least three images (100 pores) with the same magnification representing different areas of the composite were analysed at each condition.

3.3.6 Mechanical Properties

The mechanical properties of composite scaffolds reported in Table 3.1 were characterized by using a Universal Testing Machine (Shimadzu, AGS-X STD +250) (Figure 3.5). Cylindrical samples with dimensions (diameter = 13 mm ± 0.5 mm, and length = 0.9 mm ± 0.5 mm) measured using a digital calliper (J.B.S) were tested to investigate the effects of different added amounts of cross-linking agents (GP and GT) on compressive strength.

Since scaffolds for nerve regeneration must be used in the hydrated state, mechanical tests were performed in wet samples. So, prior to mechanical tests, the composite scaffolds were fully immersed into PBS for 24 h to reach equilibrium swelling as explained in 3.3.7 section. The excess water on the surface was gently removed by a filter paper.

The compression load applied during compression test was 5 N, the cross head speed was set at 1 mm/min and compressive strengths were measured at strains of 20%, 40%, and 60%. The tangent slope of the stress–strain curve, with stress (kPa) on Y-axis and deformation (%) on X-axis, was measured at 30% deformation to calculate elastic modulus. Measurements were made eight times for each composition and average values are reported.

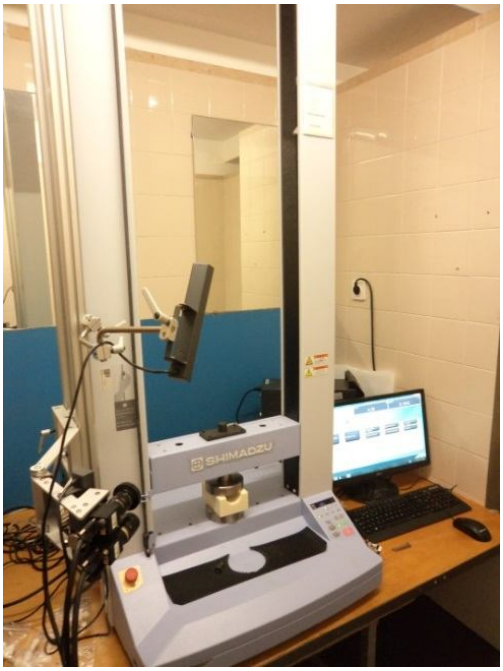

Figure 3.5. Universal testing machine (Shimadzu, AGS-X STD +250) used in this study.

3.3.7 Water Uptake (Swelling Test)

The swelling ratio is an important index used to evaluate the structural stability of the scaffolds. Because chitosan contains hydroxyl and amino groups, it is easily hydrated in water. Swelling will affect the structure of the scaffold [46].

The swelling properties of chitosan membranes were studied by immersing the previously weighted samples (un-cross-linked chitosan/FastOs®BG-Z4, and cross-linked ones with the amounts of GP and GT reported in Table 3.1 and frozen at –20ºC and –80ºC) in 10 ml phosphate buffered saline solution (PBS) (pH 7.4) at 37ºC for 24 h.

At predetermined intervals (30 min, 1, 2, 3, 12 and 24 h), the samples were withdrawn from the PBS solution, gently dried with a filter paper to remove the water adhered on the surface and then weighted. The swelling ratio (SR) of these samples was calculated by using the following equation:

$$Swelling\ ratio\ (\%) = \left[\frac{W_s - W_d}{W_d}\right] \times 100$$

where W_s and W_d are the weight of swollen samples at predetermined intervals and dry samples, respectively. Each experiment was repeated three times and the average value was taken to validate the results.

3.3.8 Weight Loss (Degradation Test)

The *in vitro* degradation of the samples was evaluated in phosphate buffered saline (PBS) solution (pH 7.4) by registering the weight loss evolution with time. The dried membranes were cut into small pieces and weighted carefully before *in vitro* analysis. The dried samples were submerged in PBS solution (1:100 w/v) and incubated at 37ºC in an incubator (Edmund Bühler GmbH) (Figure 3.6) with constant shaking (120 rpm) over indicated periods of time (2, 4, 6, and 8 weeks). PBS solution was refreshed weekly to keep a constant pH of 7.4.

Figure 3.6. The incubator (Edmund Bühler GmbH) used in this study.

Three samples of each group were removed from PBS at predetermined intervals, rinsed with distilled water and air dried in the oven at 40°C for 24 h before weight loss determination. The weight loss (W_{loss}) of specimens was calculated via following equation:

$$W_{loss}\,(\%) = \left[\frac{W_1 - W_2}{W_1}\right] \times 100$$

where W_1 and W_2 are the composite weight before and after degradation, respectively. The results reported are averages of three measurements and standard deviations were calculated.

Chapter 4

RESULTS AND DISCUSSION

4.1 Gelation Behaviour of Chitosan-based Systems

The evolution of rheological parameters (G′ and G″) of chitosan solutions with different added amounts of reticulation agents (Table 4.1) and subjected to a temperature sweep (25ºC – 90ºC, 3ºC min^{-1}) under constant oscillation conditions (frequency = 1 Hz, strain = 10^{-3}) are shown in Figure 4.1.

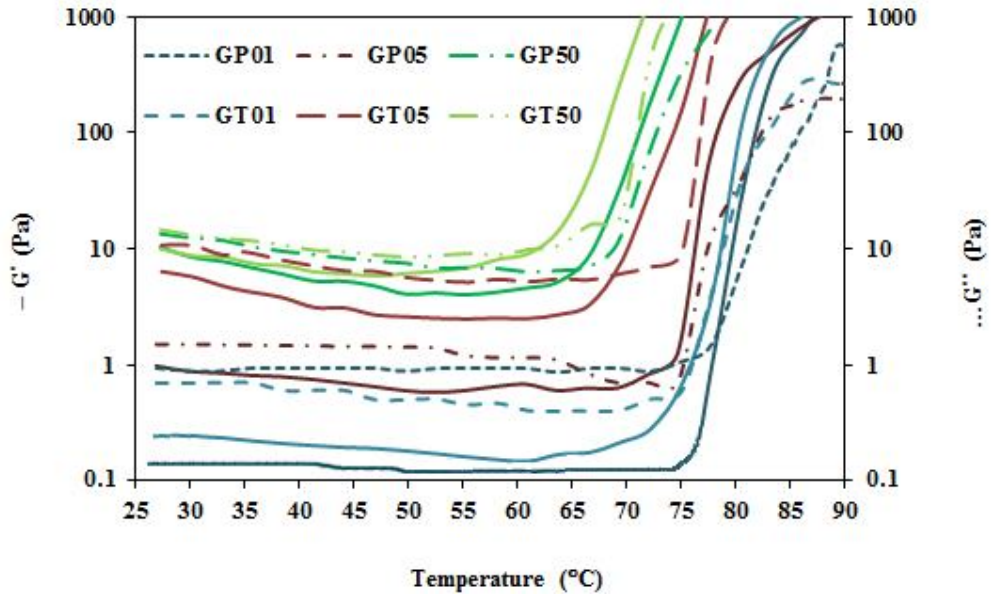

Figure 4.1. Temperature sweep for chitosan solution cross-linked with different concentrations of genipin (GP) and glutaraldehyde (GT) at different concentrations.

The curves show an initial slightly decreasing tendency with temperature increasing up to minima values that depend on the added amount and type of cross-linker used. This decreasing trend, attributed to a reduction of viscosity of the solutions with temperature rising, is followed by gradual and then abrupt slop increases as temperature further increases. This last steep increase of G′ and G″ is observed within the 60 – 80ºC range and corresponds to the temperature-induced reticulation of the systems. For a given added

amount of cross-linking agents, reticulation reactions seem to systematically occur slightly earlier in the presence of GT in comparison to GP.

The evolution of G′ and G″ for systems with added FastOs®BG-Z4 powder in the absence and in the presence of the same amounts of cross-linking agents tested for chitosan solutions are shown in Figure 4.2 and Figure 4.3, for GP and GT, respectively. Interesting features can be observed: the first descending branch of G′ and G″ curves observed in Figure 4.2 was eliminated in the presence of FastOs®BG-Z4 powder, and reticulation occurred faster than when chitosan solutions with added cross-linking agents were tested. These features can be attributed to an active reticulation role played by the surface of FastOs®BG-Z4 particles and/or by its ionic species leached to the solution.

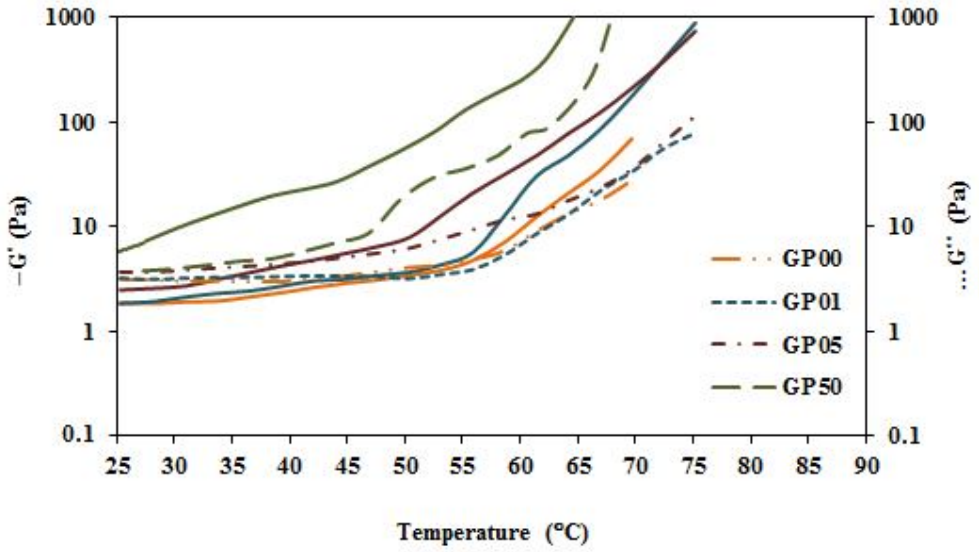

Figure 4.2. Temperature sweep for chitosan/FastOs®BG-Z4 systems cross-linked with different amounts of GP.

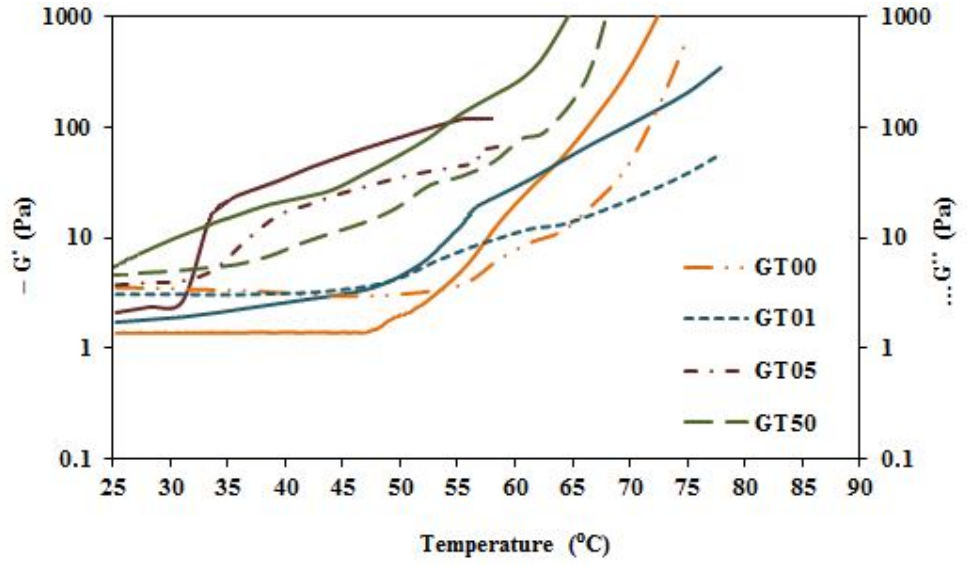

Figure 4.3. Temperature sweep for chitosan/FastOs®BG-Z4 systems cross-linked with different amounts of GT.

These observations suggest the occurrence of specific and synergetic interactions among chitosan molecules, the surface of FastOs®BG-Z4 particles and/or its ionic species leached to the solution, and the GT and GP species, which should be responsible for the observed faster gelation process. These amazing findings also suggest the possibility of preparing self-reticulation chitosan/FastOs®BG-Z4 composite scaffolds for tissue engineering, thus avoiding the use of potentially cytotoxic cross-linkers such as GT [57] [58].

This hypothesis is confirmed by the gelation temperatures estimated from all the temperature sweep tests, which are summarized in Table 4.1. It can be seen that for a given added amount of cross-liking agents, the gelation temperature of chitosan solutions was always slightly lower for GT in comparison with GP, an observation that is in good agreement with the findings reported elsewhere [75]. For composite systems, gelation always occurs at lower temperatures in comparison to the chitosan solutions, even in the absence of cross-liking agents. These findings open further research avenues that need to be explored in future studies. Gelation temperature further decreases with added GP and GT, being lowest in the presence of GT due to its enhanced reticulation ability.

Table 4.1. Estimated gelation temperatures based on temperature sweep measurements.

Gelation Temperature (°C)					
Chitosan solutions					
With added GP	GP01	~ 79	With added GT	GT01	~ 76
	GP05	~ 74		GT05	~ 67
	GP50	~ 66		GT50	~ 64
Composite systems					
With added GP	GP00	~ 50	With added GT	GT00	~50
	GP01	~ 47		GT01	~ 47
	GP05	~ 43		GT05	~ 30
	GP50	< 25		GT50	< 25

Since the control the water evaporation was difficult even when using a "solvent trap", 60ºC was selected as testing temperature for subsequent rheological characterization tests conducted under isothermal conditions.

The gelling behaviours of chitosan solutions with different added amounts GP and GT are compared in Figure 4.4, while the evolution of G′ and G″ for the system with added FastOs®BG-Z4 alone is shown in Figure 4.5.

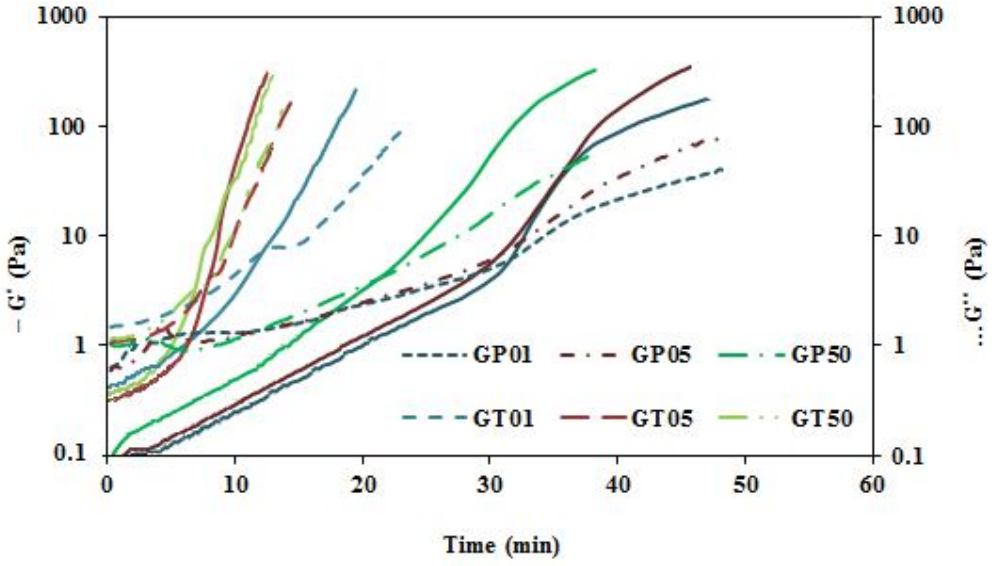

Figure 4.4. Time sweep profiles at 60°C for chitosan solution cross-linked with different added amounts of GP and GT.

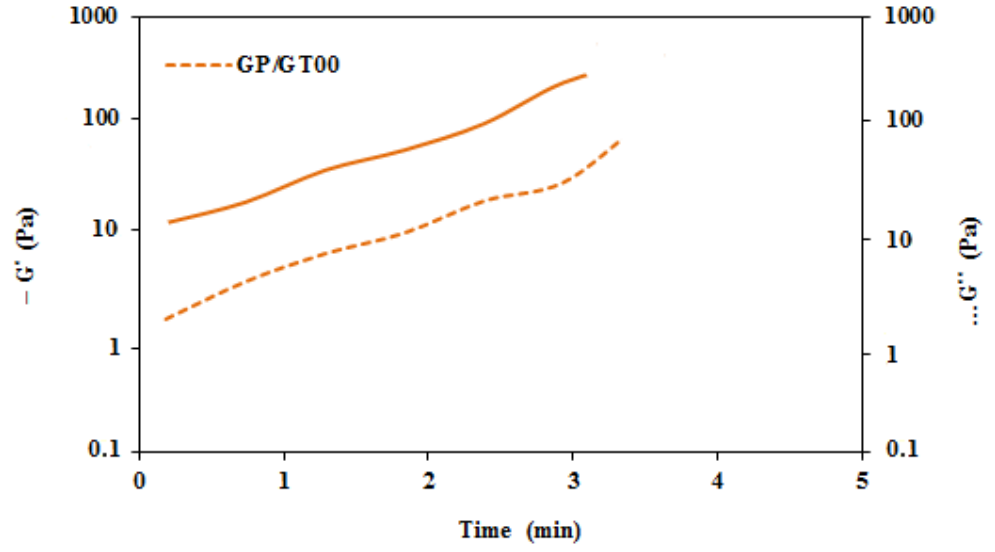

Figure 4.5. Time sweep profile at 60ºC for chitosan/FastOs®BG-Z4 system.

It can be seen that at this relatively high temperature (60ºC), reticulation started immediately eliminating any descending trend of G′ and G″ derived from temperature dependent solution viscosity, and gelation times became shorter and shorter with increasing contents of GP and GT. It is also obvious from these Figures that initially G′ < G″, with both G′ and G″ tending to increase with increasing setting time, but G′ increases faster than G″, thus leading to gelation.

The time sweep profile at 60ºC for the chitosan/FastOs®BG-Z4 system in absence of any cross-liking agent occurs much faster that when starting from chitosan solutions with different added amounts of GP and GT, as shown in Figure 4.5. Moreover, the maximum values of elastic modulus (G′) measured for this system are about two order of magnitude higher in comparison to the corresponding ones obtained from the chitosan solutions in the presence of the cross-liking agents. The estimated gelation times of chitosan solutions (Table 4.2) decrease with increasing added amounts of cross-liking agents. For a given cross-liking content, gelation times are always shorter for GT, confirming its enhanced reticulation ability in comparison to GP. No crossover point could be detected for the composite system within the experimental time frame along which G′ and G″ were measured, suggesting that cross-linking has already occurred before starting the rheological measurements.

Table 4.2. Gelation times at 60ºC for chitosan solutions cross-linked with different added amounts of GP and GT, and for the composite system without any cross-linking agent.

Gelation time (min) at 60°C (min)	
GP01	~ 32
GP05	~ 31
GP50	~ 22
GT01	~ 12
GT05	~ 8
GT50	~ 6
Chitosan/FastOs®BG-Z4 (50/50)	Already cross-linked

The results showed that only relatively weak gels could be obtained by blending 2 wt.% chitosan solution with cross-linking agents up to 0.5 wt.%, while strong gels could be quickly achieved from the composite systems even in absence of cross-linking agents, although more efficiently in their presence. Therefore, it was concluded FastOs®BG-Z4 powder has the ability to form complexes with dissociated chitosan molecules.

Chitosan contains two different kinds of functional groups, hydroxyl (*–OH*) groups and amino (*–NH_2*) groups, which are responsible for the reactivity of this polymer as an excellent natural adsorbent and give chitosan its powerful adsorptive capacity [76]. The surface adsorption mechanism would involve coulombic interactions between the positive amino groups of chitosan and the negative surface sites of FastOs®BG-Z4. Acidic pH is necessary for the protonation of amino (*–NH_3^+*) groups of chitosan. These protonated groups are likely to bind to the negatively charged surface FastOs®BG-Z4. On the other hand, hydroxyl (*–OH*) groups are also likely to form intermolecular hydrogen bonds with the surface silanol groups of FastOs®BG-Z4 powders, thus contributing to strengthen the composite gels. But the most probable gel strengthening mechanism, in the case of chitosan/FastOs®BG-Z4 composite systems, is a cationic exchange between protonated amino groups of chitosan and cationic sites onto the surface of the bioactive glass particles and/or the cationic species leached out to the solution as sketched below:

$$2\,Chit\text{–}NH_3^+ + M^{2+} \rightarrow Chit\text{–}NH_2\text{–}M\text{–}H_2N\text{–}Chit \qquad (1)$$

A similar cationic exchange mechanism could be hypothesised for the replacement of two hydronium ions from different chitosan (*Chit–OH*) molecules by a divalent cation, which would involve a decrease in pH of the media:

$$Chit\text{–}OH + HO\text{–}Chit + M^{2+}\,2H_2O \rightarrow Chit\text{–}O\text{–}M\text{–}O\text{–}Chit + 2H_3O^+ \qquad (2)$$

According to Rhazi *et al.* [77], the free amine function of chitosan confers it a better ability to chelate ions of transition metals. However, more investigations are required to

show further light on the reticulation mechanism involving the functional groups of chitosan and the surface of bioactive glass particles or the ionic species leached out to the solution.

4.2 FTIR-ATR Spectroscopy Analysis

Figure 4.6 shows the FTIR spectra within the 300–4000 cm^{-1} spectral range of FastOs®BG-Z4 powder, and of the chitosan/FastOs®BG-Z4 composite scaffolds reticulated without any added cross-linking agent, and with added 0.05 wt.% of GP or GT, all frozen at –20ºC. The aim was to identify which functional groups of chitosan would be involved in the reticulation processes undergone in the different experimental processing conditions. Unfortunately, only the limited number of samples referred above could be analysed. The spectra of LA solution and of LA+chitosan solution without and with added cross-liking agents need to be performed in future studies.

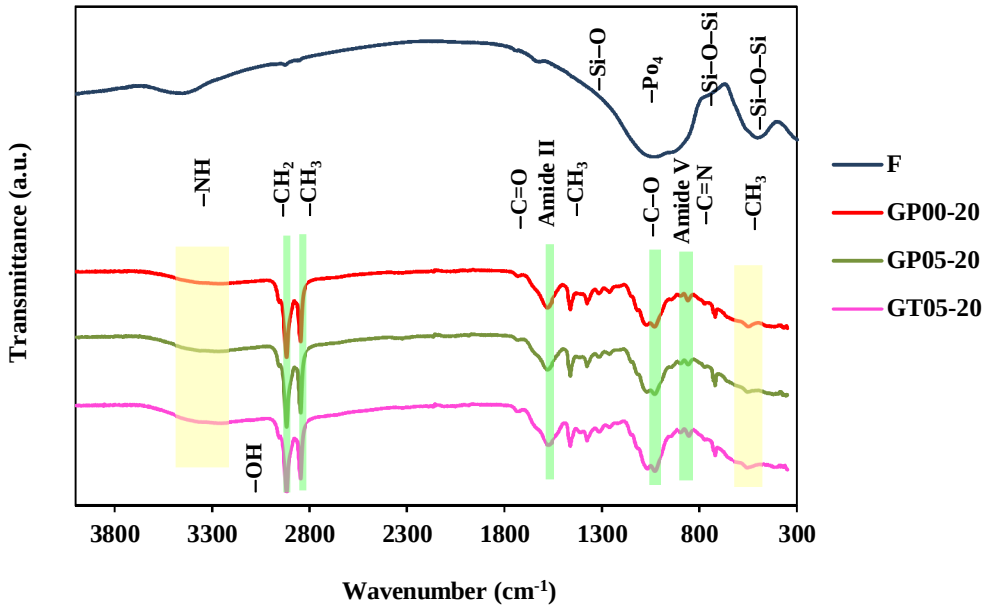

Figure 4.6. FTIR spectra of FastOs®BG-Z4 and chitosan/FastOs®BG-Z4 composites cross-linked with 0.05 wt.% of GP or GT and frozen at –20ºC.

The FTIR spectrum of FastOs®BG-Z4 exhibits three broad bands in the region of ~ 500 – 1300 cm^{-1}. The most intense bands within the 600 – 1300 cm^{-1} region correspond to the stretching vibrations of the SiO_4 tetrahedron with a different number of bridging oxygen atoms. The 800–1300 cm^{-1} region is split in two bands centred at ~1040 cm^{-1} and ~920 cm^{-1}, which can be assigned to the Si–O asymmetric stretching mode of BOs, and to the Si–O asymmetric stretching mode of the non-bridging oxygens (NBOs), respectively. Furthermore, the 510 cm^{-1} band can be attributed to Si–O–Si bending modes, while the weak 740 cm^{-1} shoulder may be due to Si–O–Si symmetric stretching with simultaneous Si cation motions. It is noteworthy that the band at 1040 cm^{-1} may also be assigned to the asymmetric stretching of PO_4 units which has been reported to appear in crystalline fluorapatite at 1038 cm^{-1} [78].

The FTIR spectra of chitosan/FastOs®BG-Z4 composites exhibit characteristic bands of chitosan. The band in the region of 3400–3500 cm^{-1} corresponds to the stretching vibration of N–H peaks at around 3480 cm^{-1} and might be also be superimposed with the absorption band due to OH group. The peaks at around 2916 cm^{-1} and 2848 cm^{-1} are assigned to CH_2 and CH_3 groups (aliphatic group). The bands at ~1660 cm^{-1} and ~1585 cm^{-1} are characteristic of respectively amide I and amide II, denoting the presence of acetyl group ($-CH_3-C=O$), so these results confirm that chitosan is partially in deacetylated form. The peaks around 1420 cm^{-1} are assigned to the CH_3 symmetrical deformation mode, and the peaks in the range of 1155 cm^{-1}, 1097 cm^{-1} and 1043 cm^{-1} correspond to the C–O stretching vibrations. Table 4.3 summarizes the FTIR data, identifying the main vibration bands and the corresponding assigned functional groups. The mentioned characteristic bands are in good agreement with data previously reported [79] [80].

The spectra of chitosan/FastOs®BG-Z4 composite systems cross-linked with GP or GT also show similar absorption bands as those identified for the composite system in absence of cross-liking agents. This suggests that the most determinant reticulation mechanisms derive from the interactions between chitosan molecules and the surface of bioactive glass particles and/or the ionic species leached thereof, with the cross-linking agents GP and GT playing secondary roles. This main conclusion is consistent with the rheological results presented in Figure 4.1– Figure 4.5, and data reported in Table 4.1– Table 4.2.

Table 4.3. Infrared frequencies of functional groups for FastOs®BG-Z4, and chitosan/ FastOs®BG-Z4 composite systems without and with adder 0.05 wt.% of GP or GT.

Wavenumber (cm^{-1})			
FastOs®BG-Z4		GP(GT)00, GP05, GT05	
600–1300	SiO_4	3480	N-H
1040	Si–O PO_4	2950	OH
920	Si–O	2916	CH_2
740	Si–O–Si	2848	CH_3
510	Si–O–Si	1660	amide I
		1585	amide II
		1420	CH_3
		1155	C-O
		1097	C-O
		1043	C-O
		750	amide V
		528	CH_3

4.3 Microstructural Analysis

The microstructure of chitosan/FastOs®BG-Z4 composites without and with added 0.01, 0.05, and 0.5 wt.% of GP or GT and frozen at –20ºC are shown in Figure 4.7– Figure 4.8. The SEM micrographs show high porosity with almost interconnected spherical pores in irregular pattern. Both the cross-linking concentration and freezing temperature seemingly affected the final porous structures of the scaffolds. Irregular porosity is mostly caused by the freeze drying and sample preparation conditions. The pores are created by the ice crystals that sublimate during freeze drying, leaving gaps or pores in their place. The pore structure corresponds to the size and shape of the ice crystals.

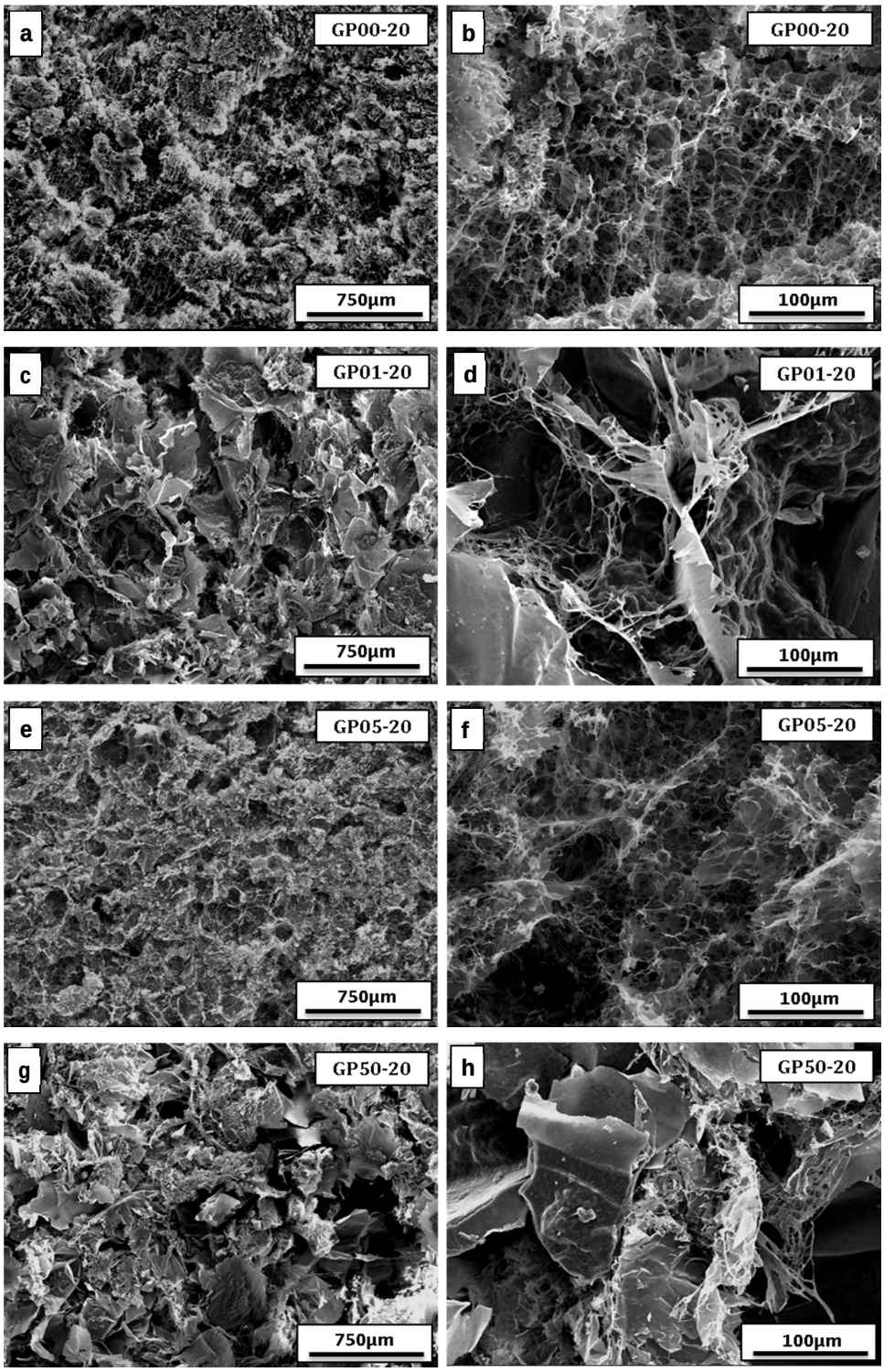

Figure 4.7. SEM micrographs of chitosan/FastOs®BG-Z4 composites frozen at –20ºC, without (a, b) and with different added amounts of GP (c, d) GP01, (e, f) GP05, (g, h) GP50.

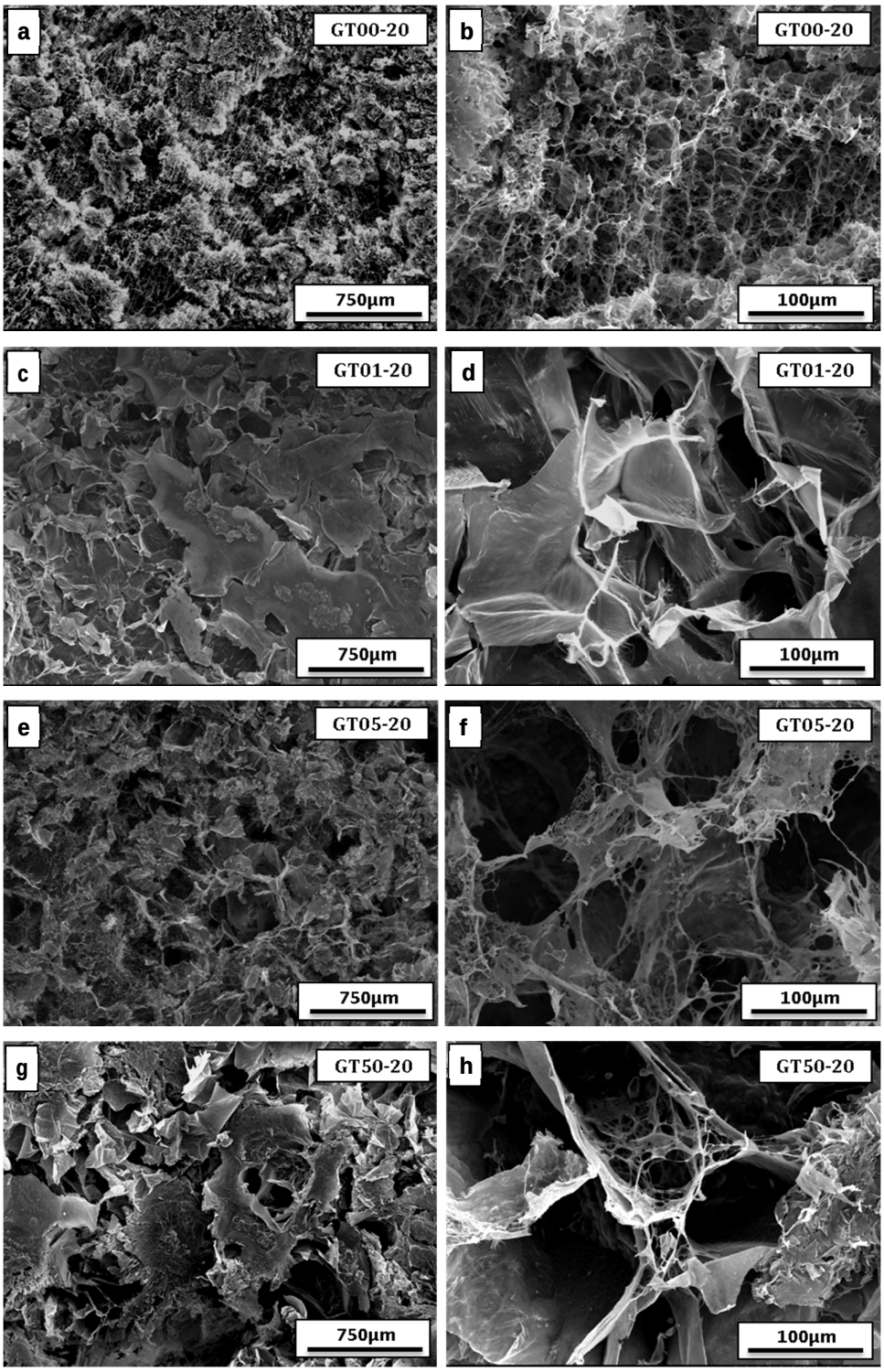

Figure 4.8. SEM micrographs of Chitosan/FastOs®BG composites frozen at –20ºC, without (a, b) and with different added amounts of GT (c, d) GT01, (e,f) GT05, (g, h) GT50.

For composites cross-linked with GP and frozen at −20ºC, Figure 4.7 shows that pore size gradually decreased from 118 ± 35 μm for 0.01 wt.% GP to 74 ± 28 μm for 0.5 wt.% GP, although the internal connectivity has been maintained. This evolution can be understood considering that an enhanced reticulation is likely to led to finer 3D porous network, and is in line with other findings reported before [73] [81]. However, there is not a complete consensus in these matters. For example, the groups of Bi [72] and Gorczyca [82] reported an increase of pore size with increasing amounts of added GP used to cross-link chitosan-collagen scaffolds. Our observations when using GP also contrast with an opposite evolution observed for the composites cross-linked with GT (Figure 4.8) in which the pore size increased from 72 ± 16 μm to 119 ± 30 μm as the GT concentration increased from 0.01 to 0.5 wt.%. All these results suggest that the pore structure is affected not only by the type and added amount of cross-linking agent but also by other experimental factors such as reticulation and freezing temperatures for polymeric solutions, and the presence inorganic components or dissolves species, the separate effects of which need to be better understood.

The effect of freezing temperature can be evaluated by comparing the SEM micrographs shown in Figure 4.9– Figure 4.10, which correspond to chitosan/FastOs®BG-Z4 composite scaffolds frozen at −20ºC and −80ºC, respectively. It is clear that scaffolds frozen at −20ºC have a more opened and spaced structure. The formation of a highly closed tight network of scaffolds at −80ºC could be explained as a result of faster gelation, which resulted in the formation of smaller ice crystals and restricted more their growth along the holding time at this temperature. At −20ºC the growth of ice crystals is facilitated by the higher kinetic energy of water molecules for diffusion.

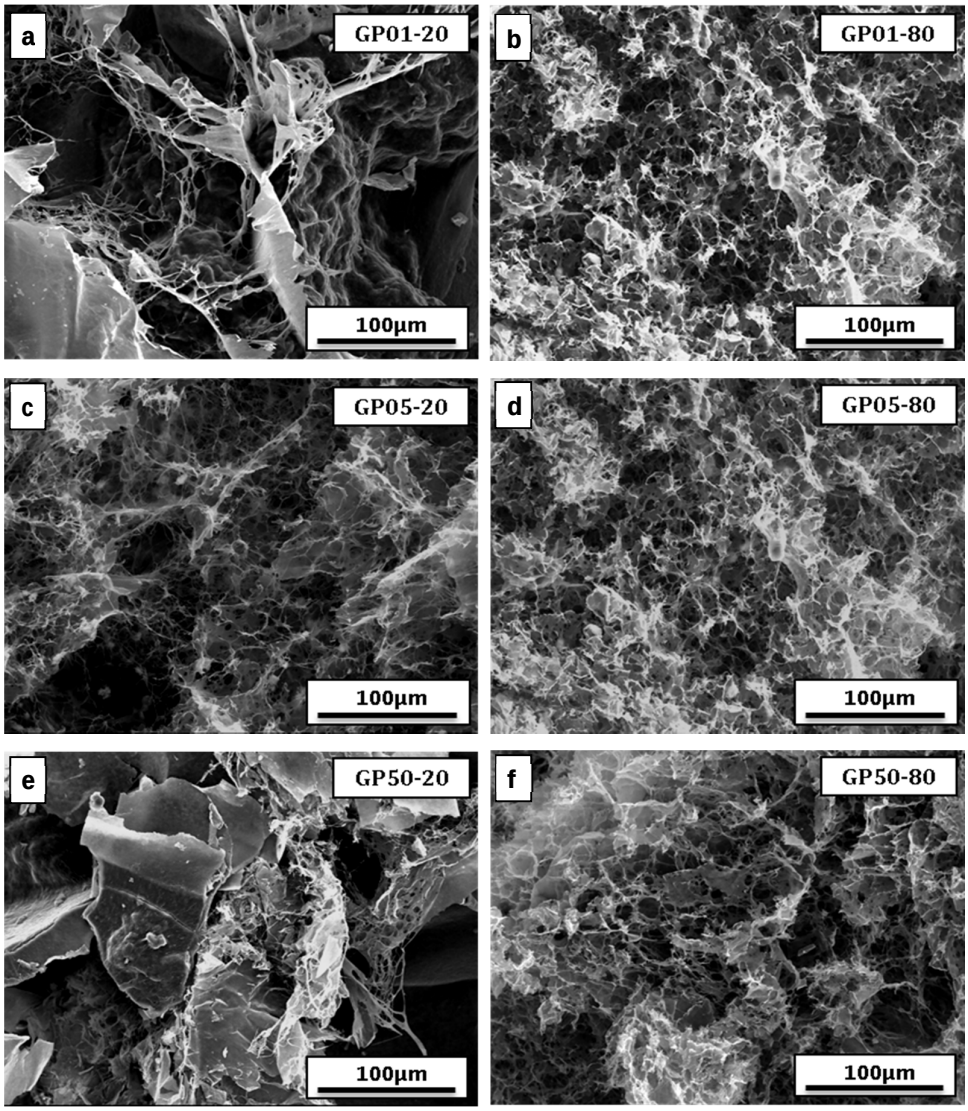

Figure 4.9. SEM micrographs of chitosan/FastOs®BG-Z4 composite scaffolds cross-linked with different added amounts of GP (a, b) GP01, (c, d) GP05, (e, f) GP50, frozen at –20ºC and –80ºC.

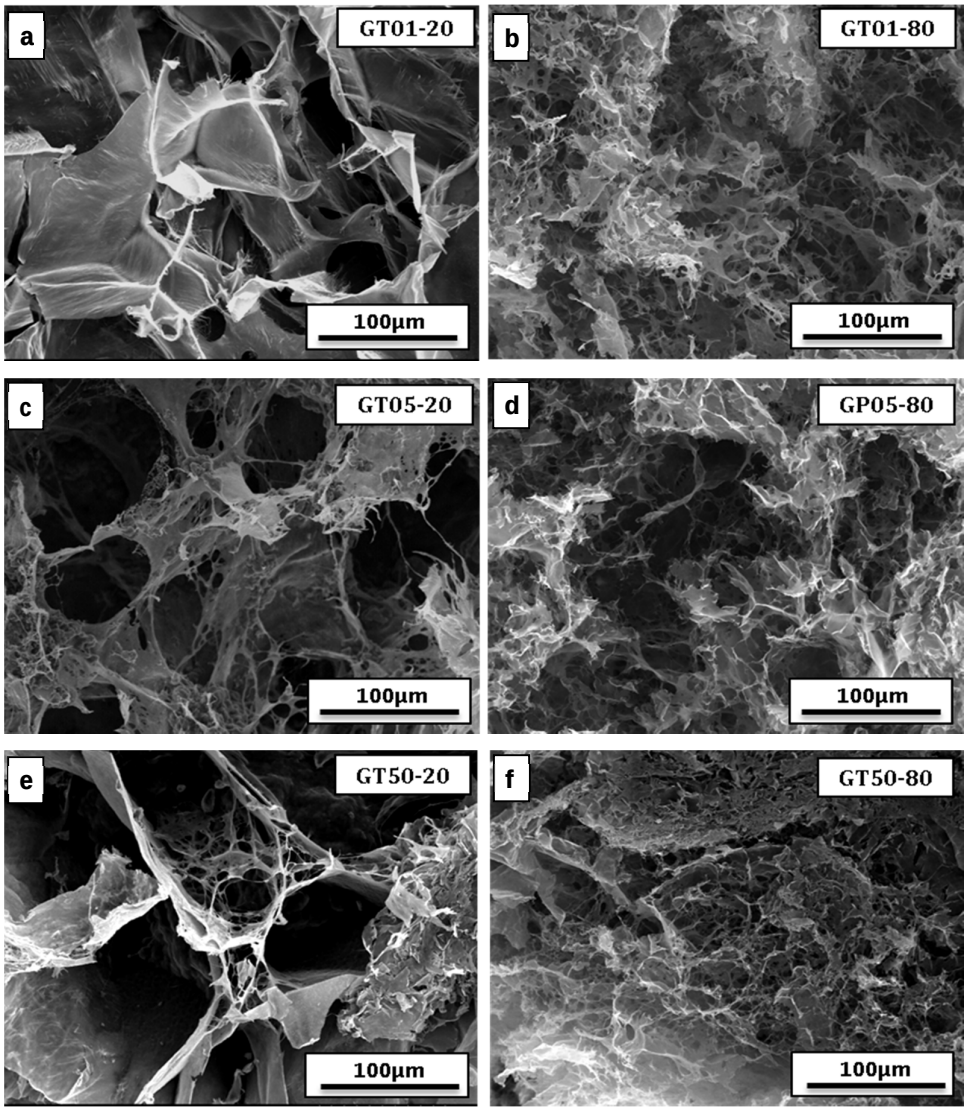

Figure 4.10. SEM micrographs of chitosan/FastOs®BG-Z4 composite scaffolds cross-linked with different added amounts of GT (a, b) GT01, (c, d) GT05, (e, f) GT50, frozen at −20ºC and −80ºC.

4.4 Cross-linking Degree Determination

The chitosan/FostOs®BG-Z4 composite scaffolds cross-linked with GT exhibited a white colour, contrasting with the typical light bluish colour obtained for those cross-linked with GP, especially with the highest added amount (GP50), as shown in Figure 4.11.

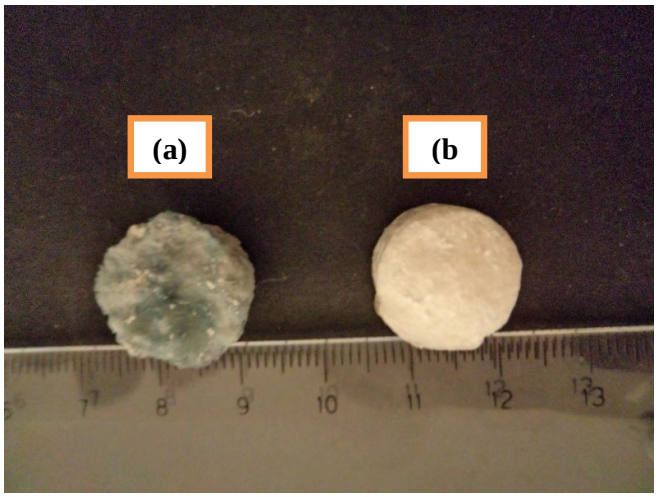

Figure 4.11. Chitosan/FastOs®BG-Z4 scaffolds cross-linked with (a) GP and (b) GT.

The cross-linking degree (CD) was determined by the ninhydrin assay [83] [84]. The concentration of free amino (NH_2) groups in the sample was determined from a standard curve of the glycine concentration versus absorbance (Figure 4.12).

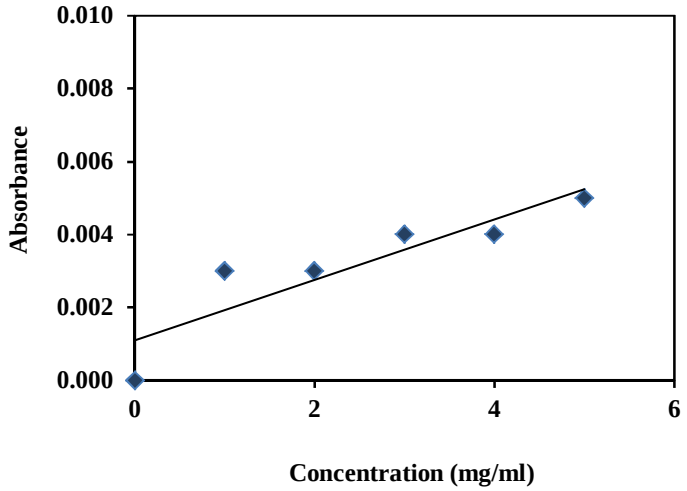

Figure 4.12. Standard calibration curve of glycine for determining unknown concentrations of ninhydrin.

The results of cross-linking degrees determined by this method are reported in Table 4.4. It can be seen that cross-linking degrees increased with increasing added amounts of GP or GT. These results confirm that GP is a less efficient cross-linker in comparison to GT, in good consistency with the finding from rheological measurements. It can be also concluded that cross-linking degree was independent of freezing temperature, in agreement with similar observations reports elsewhere [83] [84].

Table 4.4. Cross-linking degree for chitosan/FastOs®BG-Z4 scaffolds promoted by different added amounts (wt.%: 0.01; 0.05; and 0.5) of GP or GT.

Genipin	CD (%)	Glutaraldehyde	CD (%)
GP01	45.5 ± 2.7	GT01	60.2 ± 2.1
GP05	49.2 ± 2.4	GT05	65.3 ± 2.0
GP50	60.2 ± 2.5	GT50	76.2 ± 3.0

With a deacetylation degree of chitosan ≥ 85%, mean that about 85% of the repeating units of a chitosan chain have an amine group. According to the results, neither GP nor GT did utilize all available amino groups at the tested concentrations and chitosan has not been completely cross-linked. However, GT is again confirmed to be the most efficient one. Its capability to cross-link amine containing polymers by forming amine–amine bonds, so-called Schiff bases, to improved mechanical properties of scaffolds and decrease chitosan degradation in biological tissues has been widely acknowledged [85] [75]. The different cross-linking efficiencies might help explaining the differences observed in SEM micrographs of Figure 4.1– Fugure 4.5, and data reported in Table 4.1– Table 4.2.

On the other hand, GP consisting of a simple aromatic ring is not likely to produce hydrophobic p-stacking interactions with chitosan and, consequently, has a lower capability to cross-link chitosan matrix in the tested condition as compared with GT [75]. Figure 4.13 shows the schematics of chitosan cross-linking with GP and GT under near neutral conditions (pH ~ 6.8) [75].

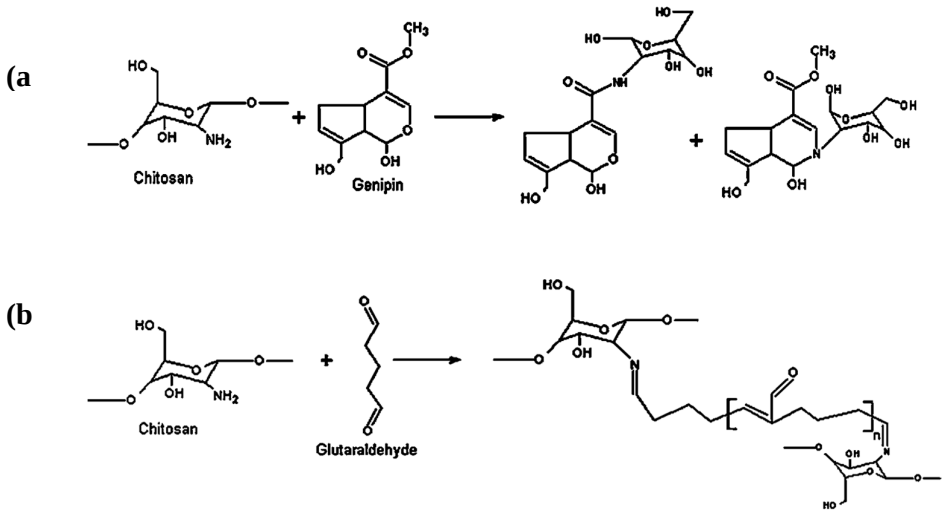

Figure 4.13. Schematic representations of the most probable chemical reactions involved at the site of free amino groups of chitosan under near neutral conditions (pH ~6.8) with (a) GP, and (b) GT [75].

According to Kil'deeva *et al.* [80], the reactivity of GT with amino groups of chitosan is different at different pH values. They have shown that in weakly acidic and neutral solutions (pH 3.0–7.2), no oligomerization is promoted by GT. At pH ≥ 5.6, the dissociation of a proton from the $OCHCH_2$ leads to the formation of an anion, the first stage of the aldol reaction. In a weakly alkaline medium (pH > 7.2) such as in the present work, GT is polymerized and the products of the aldol reaction and aldol condensation are formed, in which the polymerization rate increases with the concentration of hydroxyl ions. Increasing the pH value above 10 leads to the formation of water-soluble and -insoluble polymeric products of the aldol reaction and the condensation of GT.

In fact, the crosslinking is facilitated by formation of many irregular oligomeric glutaraldehyde molecules in which one aldehyde group of glutaraldehyde can react with chitosan while the other aldehyde group can undergo polymerization and eventually form bonds with other chitosan molecules. The mechanism leads to formation of a cross-linked structure with longer intermolecular chain lengths than would have been expected from monomeric glutaraldehyde. Formation of self-polymerized glutaraldehyde compounds, and their influence on chitosan cross-linked structures has been reported in details in some previous works [80] [86].

The cross-linking reaction mechanisms for chitosan with GP are also pH dependent. Under acidic and neutral conditions, a nucleophilic attack by the amino groups of chitosan on the olefinic carbon atom at C-3 occurs, followed by opening the dihydropyran ring of GP and attacked by the secondary amino group on the newly formed aldehyde group. In the product, short chains of condensed GP act as cross-linking bridges. Under basic conditions, the ring-opening reaction of GP occurs via a nucleophilic attack by hydroxyl ions in aqueous solution to form intermediate aldehyde groups, which subsequently undergo aldol condensation. The terminal aldehyde groups on the polymerized GP undergo a Schiff reaction with the amino groups on chitosan to form cross-linked networks. Therefore, the pH condition plays an important role in influencing the cross-linking reactions [87], which is linked to the available number of free amino groups in solution.

Under acidic environments the amino groups are essentially protonated and their participation in cross-linking process is more limited. As pH of solution increases, the number of free amino groups also increases leading to a consequent reduction in gelation time. This phenomenon is true for both GT and GP.

4.5 Pore Size and Porosity Measurement

In this study, pore sizes and porosity fractions of the composite scaffolds were evaluated using cylindrical samples of (2.4 cm diameter × 0.9 cm height) immersed into ethanol. The porosity values reported in Table 4.5 vary within the range of 80-92% depending on freezing temperature and cross-liking agent used.

Table 4.5. Porosity of chitosan/FastOs®BG membranes cross-linked with genipin and glutaraldehyde.

Composite	Porosity (%)	
	(–20ºC)	(–80ºC)
GP00/GT00	85.0 ± 2.2	80.0 ± 1.7
GP01	92.0 ± 1.0	90.0 ± 1.3
GP05	90.0 ± 1.5	88.0 ± 2.0
GP50	86.0 ± 1.7	82.0 ± 2.3
GT01	88.0 ± 1.2	85.0± 1.0
GT05	85.0 ± 1.1	83.0± 1.8
GT50	84.0 ± 1.5	80.0± 2.0

The lowest values were obtained for composite scaffolds reticulated without any added cross-liking agents, followed successively by those cross-liked with GT and GP. These results are very consistent with other data reported above, namely the obtained by rheological measurements (Figure 4.1– Figure 4.5, and Tables 4.1– Table 4.2) and cross-liking degrees (Table 4.4). All these results point out to an apparent enhanced reticulation efficiency of chitosan with added FastOs®BG-Z4 powder in comparison to the chitosan solutions with added GT and GP. For an easier visualization, the porosity data of composites scaffolds cross-linked with GP and GT have also been plotted in Figure 4.14 to Figure 4.17 aiming at better comparing the separate effects of cross-likers and freezing temperatures.

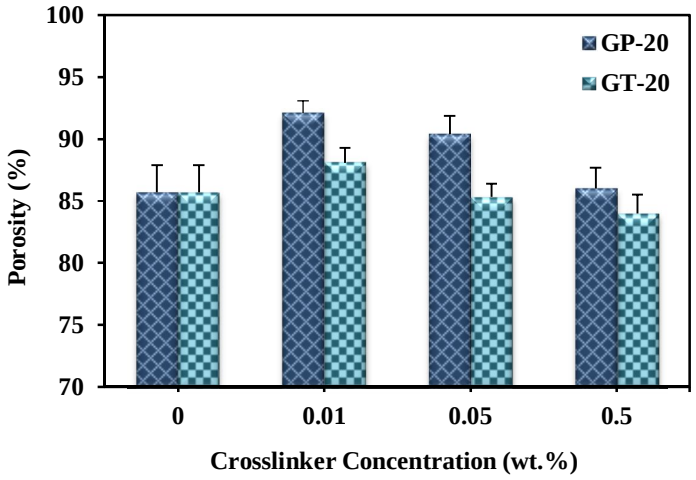

Figure 4.14. Percentage of porosity of composite scaffolds frozen at −20ºC cross-linked by GP or GT.

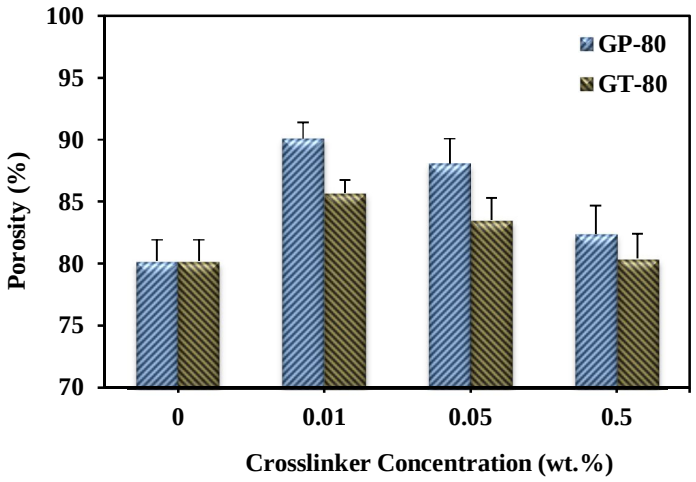

Figure 4.15. Percentage of porosity of composite scaffolds frozen at −80ºC cross-linked by GP or GT.

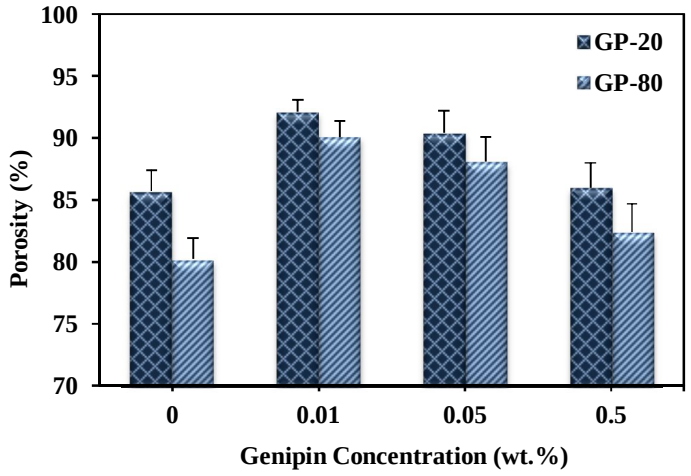

Figure 4.16. Effect of freezing temperature on the percentage of porosity of composite scaffolds cross-linked GP.

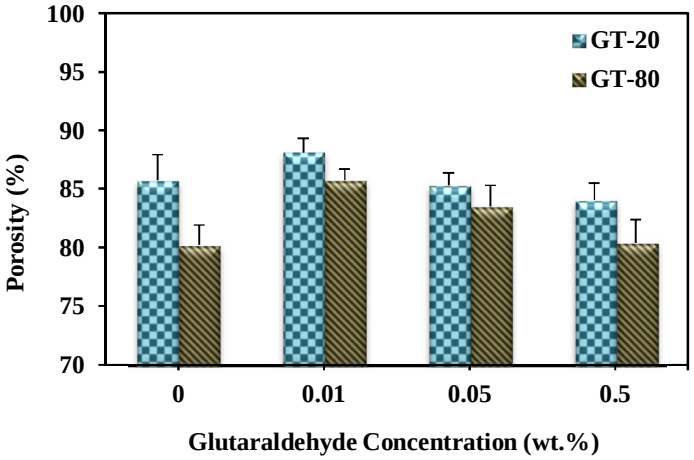

Figure 4.17. Effect of freezing temperature on the percentage of porosity of composite scaffolds cross-linked GT.

From Table 4.5 and Figure 4.14 to Figure 4.17, it can be clearly seen that under all the reticulation conditions tested, the composite scaffolds frozen at –80ºC are systematically

less porous in comparison to the samples frozen at −20ºC, an observation that is consistent with the more favourable temperature induced growing of ice crystals at −20ºC, and with the microstructural features observed in SEM micrographs (Figure 4.7 to Figure 4.10). The overall results observed in the present work are in good agreement with findings reported by Shirosaki [88], Ren [89], Kang [90] and Ho [91].

The larger pores will provide space for the migration of cells and to improve the diffusion of nutrients and metabolites throughout the membrane [81]. Some reports point out that multi-channel conduits with relatively higher porosity and greater average channel diameters could provide a more permissive environment for axonal ingrowth than those having lower porosity and smaller average channel diameters [92] [93]. The adhesion and proliferation of cells are influenced by porosity so this is a decisive factor for absorption ability of scaffolds. High porosity and interconnectivity pore structure are necessary for tissue-guided scaffold materials. The pore diameter should be in the range of cell diameters to enable cell infiltration and vascularization of the scaffold [94]. Chitosan membranes with about 90% porosity and average pore size of ~110 μm were reported to significantly improve nerve fibre regeneration and the degree of functional recovery [95]. In other study done by Wan *et al.* [96] the porosity and average channel diameter of the conduits were respectively set as around 80% and 200 μm by controlling processing parameters with required mechanical strength and degradation rates. In addition, it has also been observed that the channels inside conduits would be blocked due to swelling of the conduits if the channel diameters are too small, resulting in no nerve growth in the blocked conduits [93].

4.6 Mechanical Properties

Hydrated porous chitosan/FastOs®BG-Z4 composite scaffolds were soft, spongy and very flexible. No maximum compression strength was obtained because the scaffolds did not break when subject to compression up to strain values of ~60%, the maximum value used for all the samples. The date plotted in Figure 4.18– Figure 4.21 are intended to convey an easy visualization of the separate effects of added cross-likers and freezing temperatures on the mechanical properties of chitosan/FastOs®BG-Z4 composite scaffolds.

Generally, the mechanical compressive strength values of the cross-linked chitosan scaffolds always increases with increasing added amounts of cross-linking. The only exception was observed for the highest added amount of GT. This deviation from the main trend can be attributed to the concomitant increase of the average size of pores formed under these conditions. The smaller average pore sizes formed in samples frozen at –80ºC can also explain the systematically higher compressive strength values registered for these samples in comparison to those obtained from samples frozen at –20ºC. The same argument is also valid when comparing the compressive strength values of composite scaffolds reticulated with different cross-linking agents. The higher percentages of porosity measured for scaffolds cross-linked with GP (Table 4.6), coupled with the larger pores observed for these scaffolds (Figure 4.7 and Figure 4.8) support the registered compressive strength data plotted in Figure 4.18– Figure 4.21.

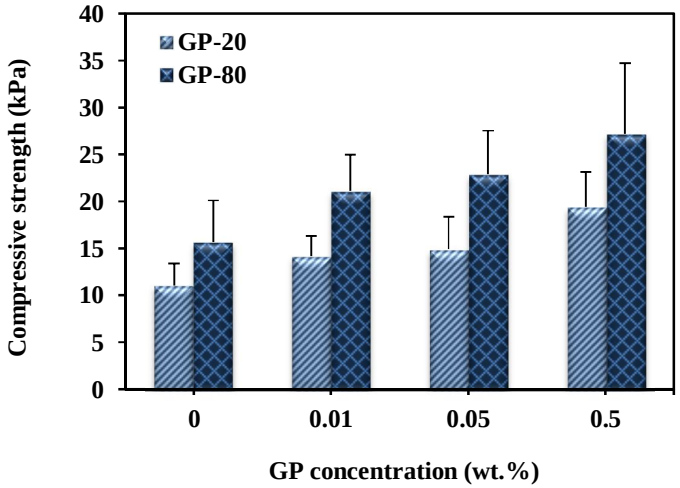

Figure 4.18. Compressive strength of chitosan/FastOs®BG-Z4 composite scaffolds cross-linked with GP.

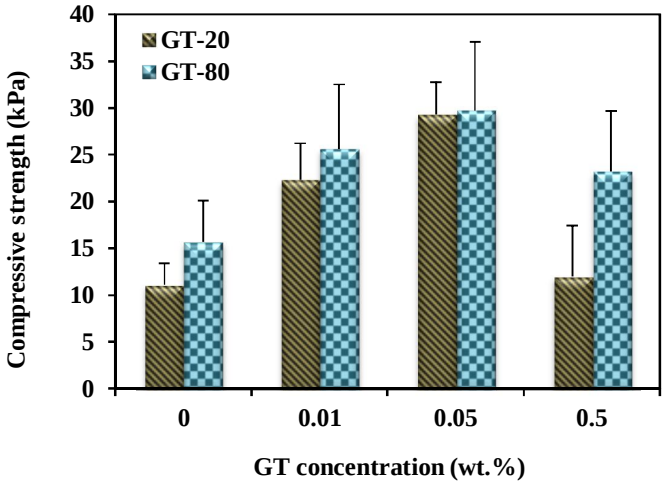

Figure 4.19. Compressive strength of chitosan/FastOs®BG-Z4 composite scaffolds cross-linked with GT.

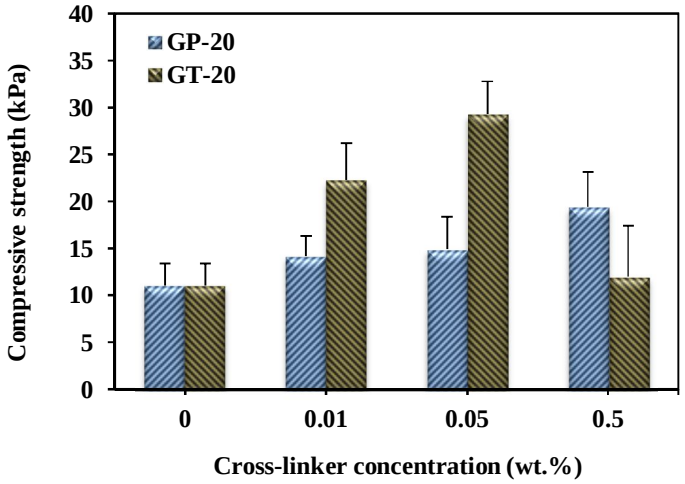

Figure 4.20. Compressive strength of chitosan/FastOs®BG-Z4 composite scaffolds cross-linked with GP and GT frozen at –20ºC.

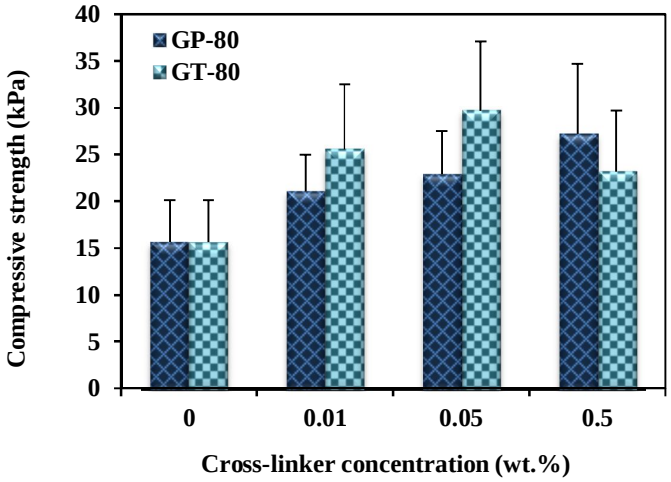

Figure 4.21. Compressive strength of chitosan/FastOs®BG-Z4 composite scaffolds cross-linked with GP and GT frozen at –80ºC.

Another interesting and expected feature is the increasing trend observed for compressive strength with increasing strains. To better illustrate such evolution compressive strength values were registered for all composite scaffolds at strains of 20%, 40%, and 60%. The date was plotted in Figure 4.22– Figure 4.25. These results confirm the above referred general increasing trend of compressive strength with increasing added amounts of cross-liking agents, at both freezing temperatures (–20ºC and –80ºC), with the exception of the highest amount of GT (Figure 4.24 and Figure 4.25) that led to the formation of larger pores as confirmed by the SEM micrographs (Figure 4.8 and Figure 4.10).

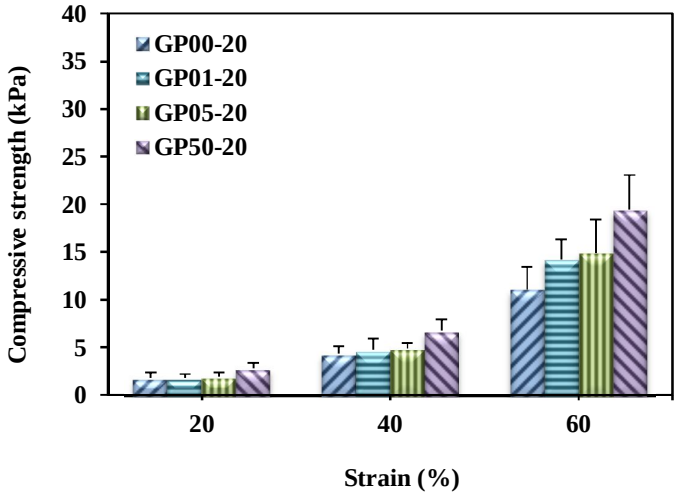

Figure 4.22. Evolution of compressive strength with strain for composite scaffolds frozen at –20ºC, cross-linked without and with different added amounts of GP.

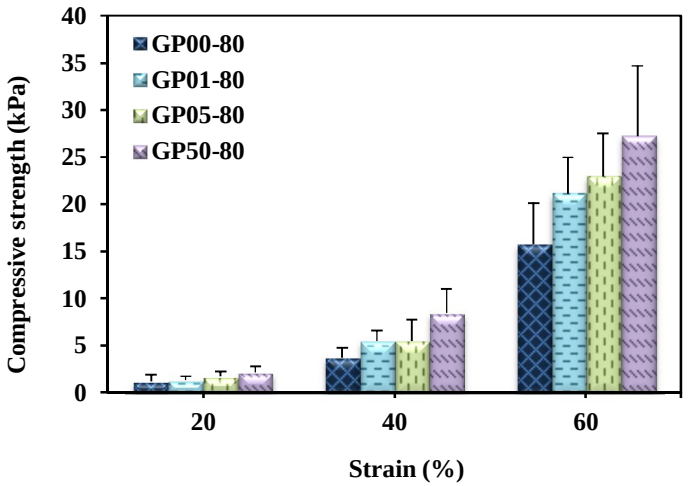

Figure 4.23. Evolution of compressive strength with strain for composite scaffolds frozen at –80ºC, cross-linked without and with different added amounts of GP.

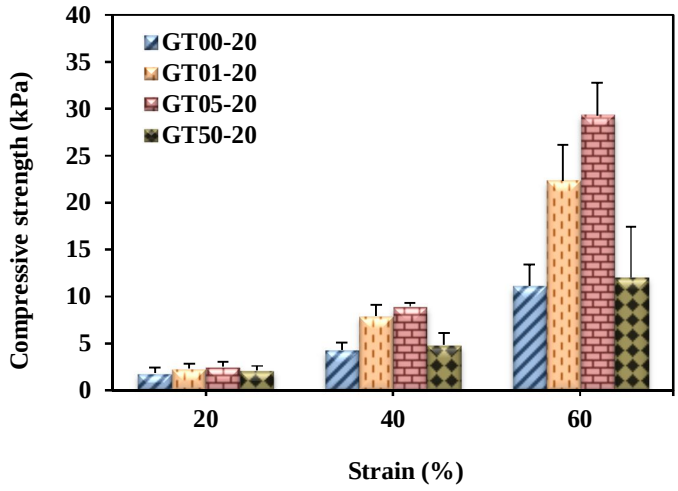

Figure 4.24. Evolution of compressive strength with strain for composite scaffolds frozen at –20ºC, cross-linked without and with different added amounts of GT.

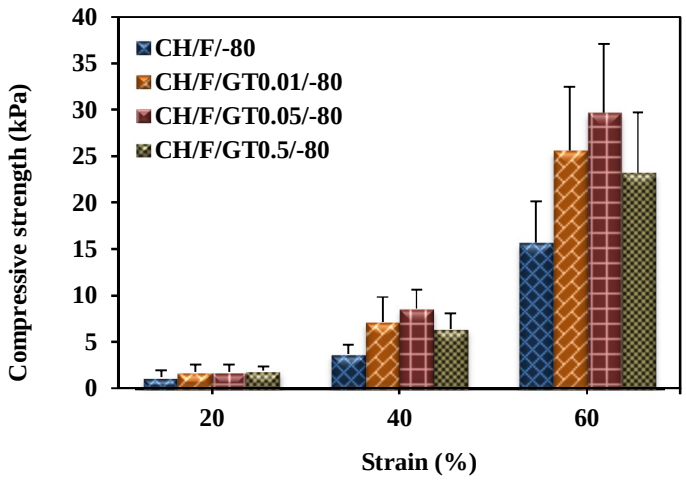

Figure 4.25. Evolution of compressive strength with strain for composite scaffolds frozen at –80ºC, cross-linked without and with different added amounts of GT.

Many factors affect the gelling time and the final structural and mechanical properties of scaffolds made of polymers or of composite systems, including the concentration of constituting components and of cross-linking agents, the solvent composition, the processing (cross-linking and freezing temperatures), etc. [97] [98] [99]. The results reported above and in previous literature reports clearly indicate that compressive strength of porous scaffolds is mainly dependent on pore structure. The same arguments are valid for the elastic modulus values that were plotted in (Figure 4.26 to Figure 4.29).

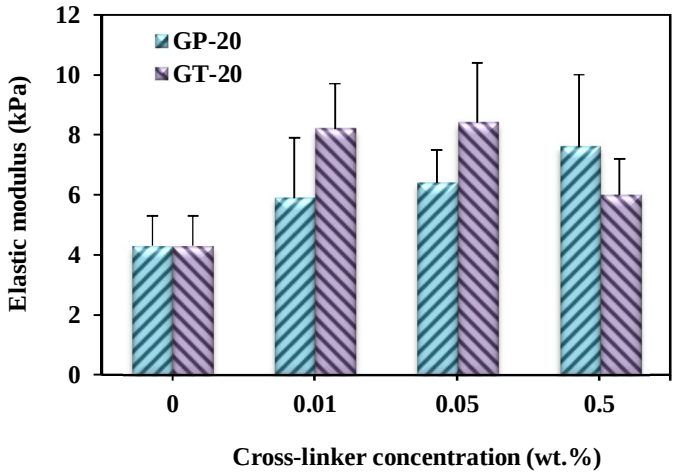

Figure 4.26. Elastic modulus of chitosan/FastOs®BG-Z4 composite scaffolds cross-linked without and with different added amounts of GP and GT, frozen at –20ºC.

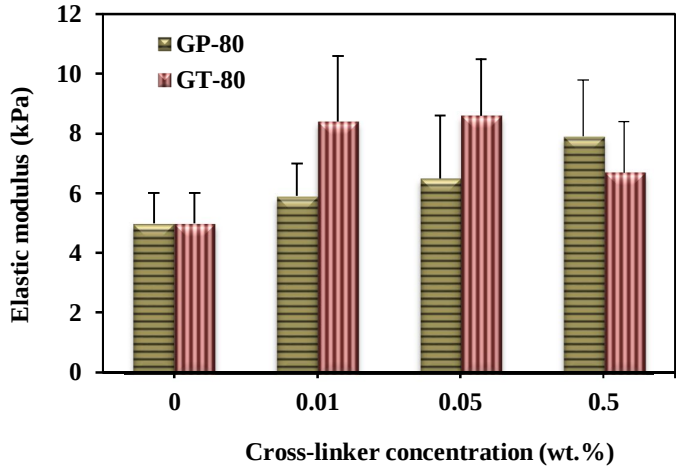

Figure 4.27. Elastic modulus of chitosan/FastOs®BG-Z4 composite scaffolds cross-linked without and with different added amounts of GP and GT, frozen at –80ºC.

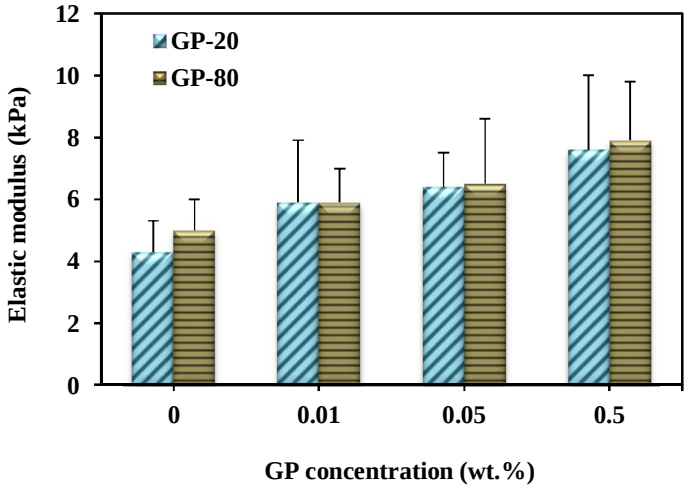

Figure 4.28. Elastic modulus of chitosan/FastOs®BG-Z4 composite scaffolds cross-linked without and with different added amounts of GP, frozen at −20ºC and −80ºC.

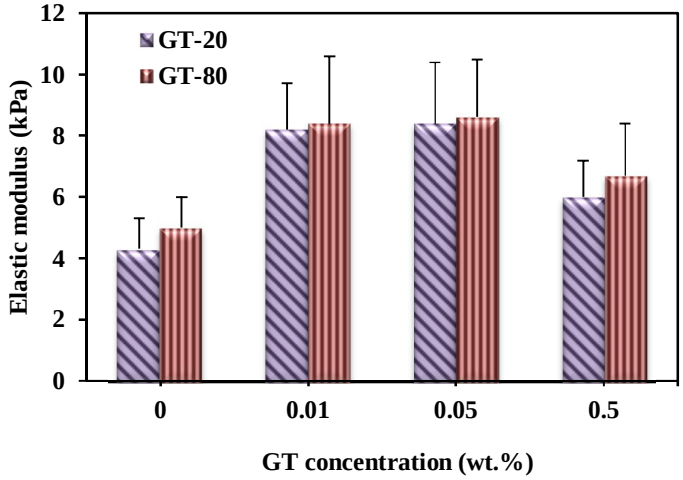

Figure 4.29. Elastic modulus of chitosan/FastOs®BG-Z4 composite scaffolds cross-linked without and with different added amounts of GT, frozen at −20ºC and −80ºC.

It seems consensual that smaller pores and higher cross-linking degrees are helpful to enhance the biomechanical strength engineered constructs [72]. It is also recognized that appropriate mechanical properties are required for nerve scaffolds to remain intact during a suture process and provide a temporary mechanical support sufficient to withstand in vivo

forces exerted by the surrounding tissues [100]. Hence, in order to yield ideal polymer scaffolds, the optimal crosslinking condition should be investigated.

Nerve conduits with enough mechanical properties will resist muscular contractions and maintain structural support with enough space and stability to facilitate nerve regeneration [35]. The enhanced mechanical properties of chitosan/FastOs®BG-Z4 composite membranes will allow better shape stability in comparison to those made from chitosan alone, making them more promising for these biomedical applications.

4.7 Swelling Behaviours

The swelling ratio is an important index used to evaluate the structural stability of a biodegradable scaffold. The swelling should be moderate. If too great, the scaffold will swell much in vivo, decreasing the available space the biological processes to occur within the scaffold. If too poor, it will cause local hydropenia at the implanting site [49]. As shown in Figure 4.30 to Figure 4.33, the scaffolds with added cross-linking agents exhibit a higher swelling capacity in comparison to that obtained without cross-linkers.

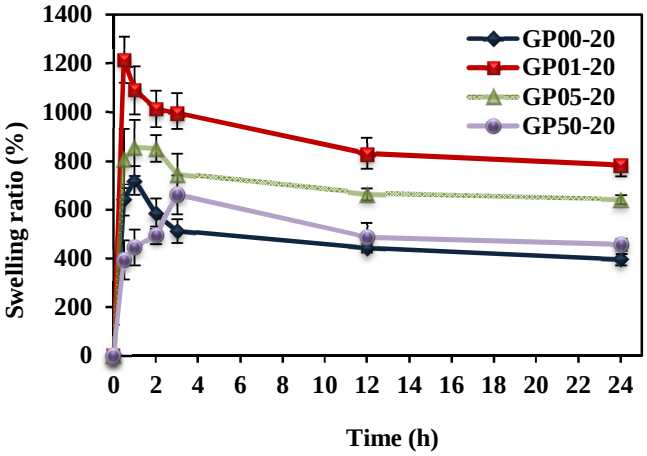

Figure 4.30. Swelling ratio of chitosan/FastOs®BG-Z4 composite scaffolds cross-linked without and with different added amounts of GP, frozen at –20ºC.

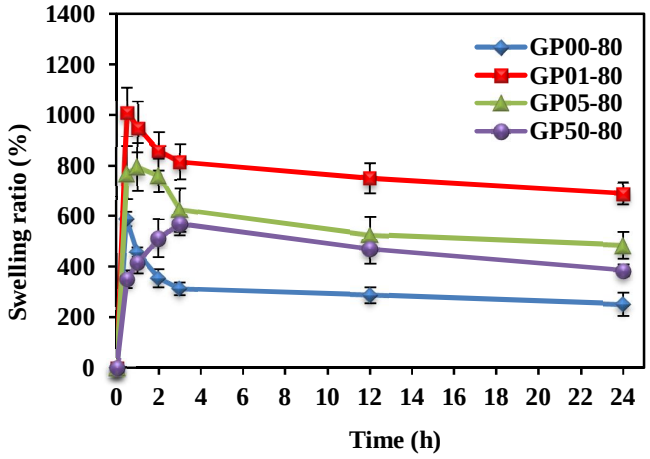

Figure 4.31. Swelling ratio of chitosan/FastOs®BG-Z4 composite scaffolds cross-linked without and with different added amounts of GP, frozen at –80ºC.

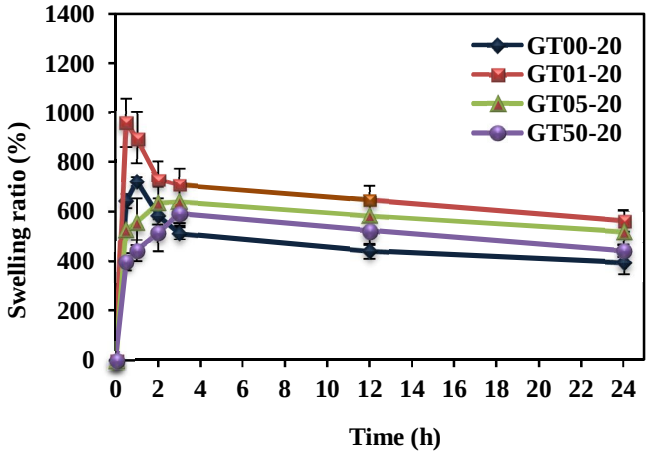

Figure 4.32. Swelling ratio of chitosan/FastOs®BG-Z4 composite scaffolds cross-linked without and with different added amounts of GT, frozen at –20ºC.

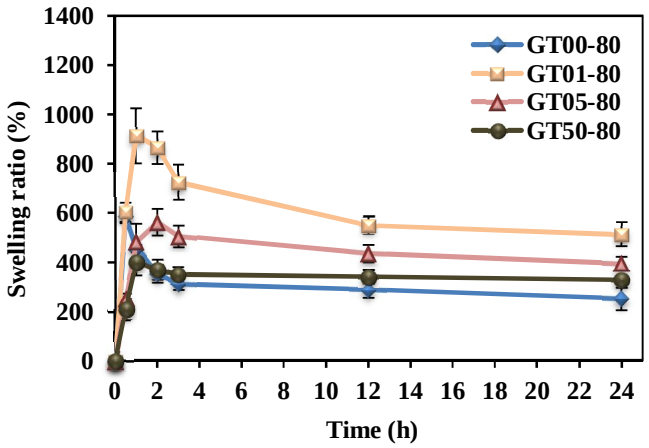

Figure 4.33. Swelling ratio of chitosan/FastOs®BG-Z4 composite scaffolds cross-linked without and with different added amounts of GT, frozen at –80ºC.

The swelling data plotted in Figure 4.30 to Figure 4.33 show an abrupt initial increase of PBS solution uptake followed by an accentuated decreasing trend up to about 3 h, and then by a slow and steadily decreasing along the remaining testing time interval (up to 24 h). It can be seen that the less swelling capacity was obtained in the absence of cross-liking agents, followed by the samples with the highest amounts of GP and GT. The differences observed among the samples are consistent with the measured percentages of porosity (Table 4.5). In addition, the volume or shape of all scaffolds scarcely changed during soaking in PBS. The scaffolds absorbed PBS solution without collapsing of the 3D pore structure.

The swelling properties of porous chitosan-based scaffolds can be understood based on the hydrophilic and cationic character of this polymer. Besides porosity, cross-linking of chitosan can also change its hydrophilicity, which, in turn will further decrease the swelling ratio scaffold [101]. Therefore, it can be concluded that the swelling behaviour of the composite chitosan/FastOs®BG-Z4 membranes and their mechanical stability are mostly determined by the porous structure and the relevant factors behind it (the kind and the added amount of cross-linker, and processing temperatures). Similar conclusions were drawn by Bi *et al.* group [72] for chitosan scaffolds.

4.8 Degradation Behaviours

The degradation rate is another important index for the evaluation of scaffolds. The weight loss (*WL*) of the chitosan/Fastos®BG-Z4 composite scaffold without any added cross-linking agent was used as a control to compare with the others cross-linked with different added amounts of GP or GT.

The *WL* data of all the chitosan/Fastos®BG-Z4 composite scaffolds are presented in Figure 4.34 to Figure 4.37 as a function of immersion time.

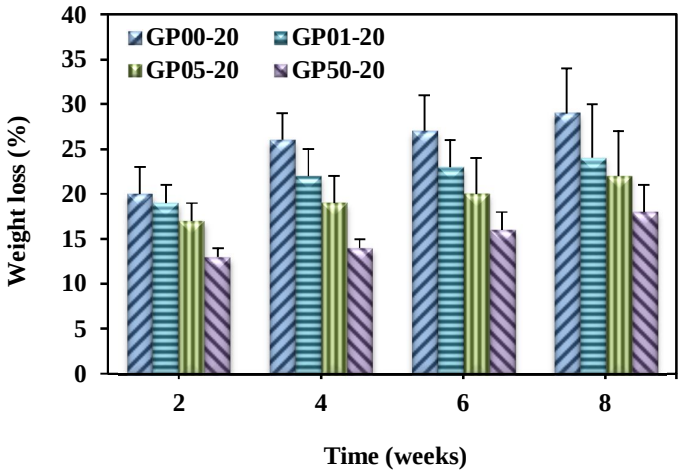

Figure 4.34. Percentage of weight loss for chitosan/FastOs®BG-Z4 composite scaffolds cross-linked without and with different added amounts of GP, frozen at −20ºC.

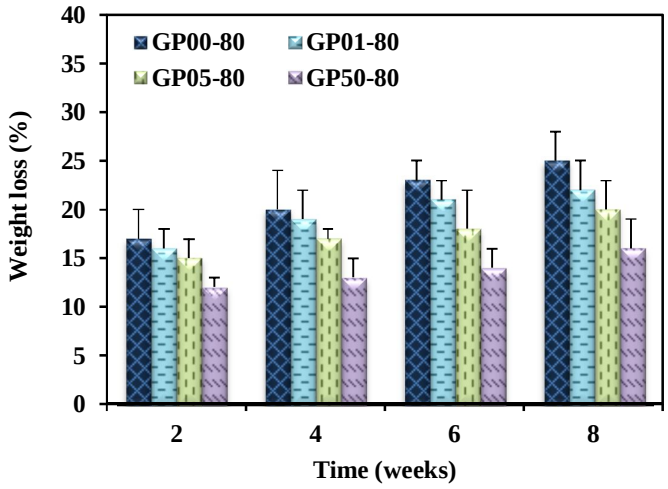

Figure 4.35. Percentage of weight loss for chitosan/FastOs®BG-Z4 composite scaffolds cross-linked without and with different added amounts of GP, frozen at −80ºC.

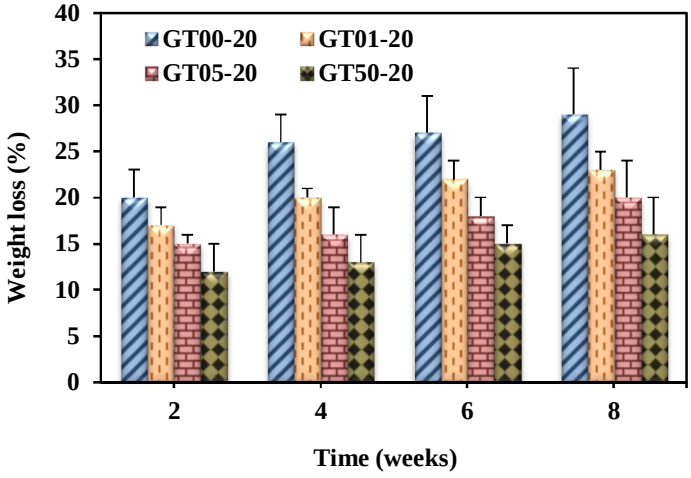

Figure 4.36. Percentage of weight loss for chitosan/FastOs®BG-Z4 composite scaffolds cross-linked without and with different added amounts of GT, frozen at −20ºC.

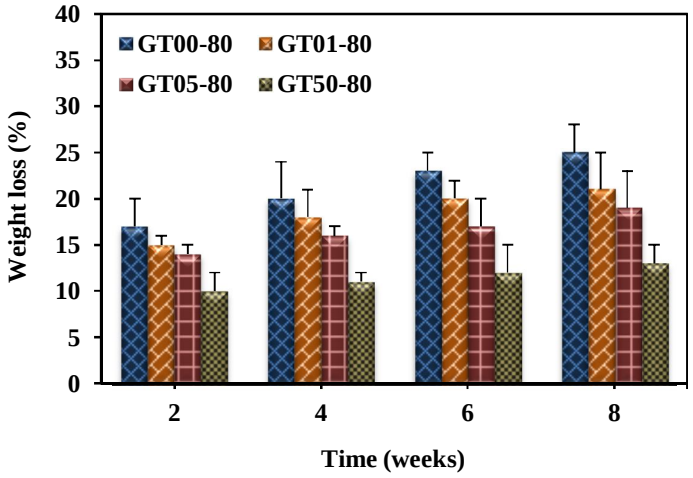

Figure 4.37. Percentage of weight loss for chitosan/FastOs®BG-Z4 composite scaffolds cross-linked without and with different added amounts of GT, frozen at –80ºC.

.

From these Figure 4.34– Figure 4.37, it can be seen that the degradation rates decrease with increasing added amounts of cross-linking agents at constant pH = 7.4, with the highest values being observed for the control sample reticulated without any added cross-linker. Another important conclusion is that degradation rates are systematically slower for samples frozen at the lower freezing temperature (–80ºC).

This expected behaviour is eventually more easily observed when degradation data of chitosan/FastOs®BG-Z4 composite scaffolds cross-linked with GP or GT, collected after soaking for 8 weeks in PBS solution is plotted against the added amounts of cross-linking agents, as shown in Figure 4.38 and Figure 4.39.

The results observed are according to the cross-linking degree detected by the NHN assay. The higher crosslinking degrees promoted by GT (Table 4.4) resulted in systematic lower weight losses. Regardless of the presence, or not, of cross-linking agents and of the weight losses undergone, all composite scaffolds maintained their structural integrity, an essential feature for successful applications in nerve repair.

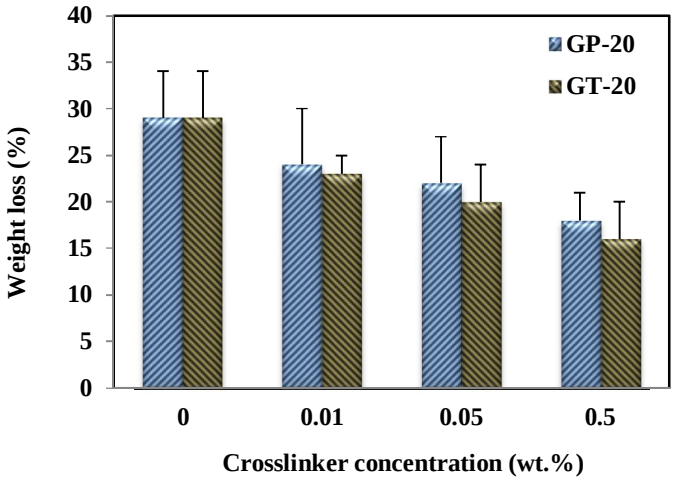

Figure 4.38. Percentage of weight loss after 8 weeks soaking in PBS solution of chitosan/ FastOs®BG-Z4 composite scaffolds cross-linked without and with different added amounts of GP and GT, frozen at –20ºC.

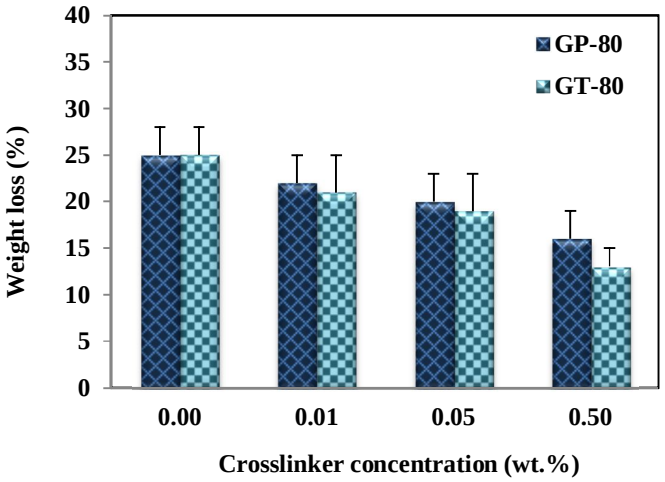

Figure 4.39. Percentage of weight loss after 8 weeks soaking in PBS solution of chitosan/ FastOs®BG-Z4 composite scaffolds cross-linked without and with different added amounts of GP and GT, frozen at –80ºC.

Chapter 5

Conclusions

The results obtained along this Master thesis project enable a number of conclusions to be drawn, the most salient one is the disclosure for the first time that self-setting chitosan/FastOs®BG-Z4 porous composite scaffolds/membranes can be prepared by just adding the bioactive glass particles to the chitosan solutions. Although the setting/reticulation mechanism still demands further investigations to become fully understood, it was hypothesized that both active sites at the surface of bioactive glass particles and the ionic species leached off to the solution are likely to play a cross-liking role. These amazing findings mean that the use of potentially cytotoxic cross-linkers such as GT can be avoided, thus making the membranes for nerve regeneration innocuous and bio-friendly.

Besides this main important achievement, several other specific conclusions can be drawn from the present work as detailed below:

1. The naturally occurring genipin (GP) and the traditional synthetic glutaraldehyde (GT) revealed to be suitable cross-linkers for making 3D composite chitosan/FastOs®BG-Z4 porous membranes for nerve regeneration. The cross-linking efficiency and the consequent mechanical stability are generally higher in the case of GT in comparison to GP, except for the highest added amount of GT.

2. The enhanced cross-linking efficiency of GT resulted in higher cross-linking degrees and systematic lower percentages of porosity and swelling ratios, and slower degradation rates upon immersion in PBS solution, as expressed by the undergone weight losses along a time period of 8 weeks. Accordingly, the higher degradation rates were observed for the self-reticulated porous chitosan/FastOs®BG-Z4 composite membranes.

3. For both cross-linking agents used, the cross-linking degree always increased with the added amounts, within the range of concentrations tested, with direct reflexes in terms of the overall properties of the resulting scaffolds.

4. The lower freezing temperature (–80ºC) revealed to be more effective in decreasing the pore size and porosity fraction, thus enhancing the mechanical properties and the stability of the scaffolds when submitted to swelling and degradation tests.

5. The freezing temperature of –20ºC was selected as the most suitable one when considering the porous microstructural features and the intended applications.

6. Regardless of the presence, or not, of cross-linking agents and of the weight losses undergone, all composite scaffolds maintained their structural integrity, an essential feature for successful applications in nerve repair.

Chapter 6

Future Work and Recommendations

The most salient finding of the present work opened further research avenues that need to be explored in future studies. The self-reticulation mechanism of chitosan/Fastos®BG-Z4 needs to be investigated in detail in order to clarify the relative importance of the surface chemistry of the bioactive glass particles and of the dissolves ionic species. It would be also important studying the influence of different chitosan/Fastos®BG-Z4 weight ratios on the gelation process and on the overall properties of the resulting scaffolds.

Obviously, testing the scaffolds *in vitro* for cytotoxicity, biocompatibility and cell proliferation, and *in vivo* are essential steps to be conducted in the future to evaluate the suitability of the composite membranes for the intended clinical applications as nerve guides in peripheral nerve regeneration.

List of References

[1] N. Cao, "Master Thesis: Fabrication of Alginate Hydrogel Scaffolds and Cell Viability in Calcium-Crosslinked Alginate Hydrogel," University of Saskatchewan, 2011, p. Chapter 1.

[2] M. Haugh, "PhD Thesis: The Development of Novel Scaffolds for Tissue Engineering with a Range of Structural and Mechanical Properties," Trinity College, 2009.

[3] S. Güven, "Master Thesis: Integrated Biomimetic Scaffolds for Soft Tissue Engineering," Middle East Technical University, School of Natural and Applied Sciences, 2006, p. Chapter 1.

[4] B. Lawrence, "Master Thesis: Composite Scaffolds of Natural and Synthetic Polymers for Bladder Tissue Engineering," Oklahoma State University, School of Chemical Engineering, p. Chapter 1.

[5] M. Lee, J. Dunn and B. Wu, "Scaffold fabrication by indirect three-dimensional printing," *Biomaterials,* vol. 26, no. 20, pp. 4281-4289, 2005.

[6] C. Schmidt and J. Leach, "Neural tissue engineering: strategies for repair and regeneration," *Annual Review of Biomedical Engineering,* vol. 5, pp. 293-347, 2003.

[7] J. B. Recknor and S. K. Mallapragada, "Nerve Regeneration: Tissue Engineering Strategies," in *The Biomedical Engineering Handbook: Tissue Engineering and Artificial Organs,* 3 ed., J. Bronzino, Ed., new York, Taylor & Francis, 2006, p. Chapter 48.

[8] A. Gärtner, "PhD thesis: Association of biomaterials and mesenchymal stem cells from Wharton's jelly of human umbilical cord for promotion of peripheral nerve regeneration: A functional and morphological study," University of Porto, 2013.

[9] X. Gu, F. Ding, Y. Yang and J. Liu, "Construction Tissue Engineered Nerve Grafts and Their Application in Peripheral Nerve Regeneration," *Progress in Neurobiology,*

vol. 93, pp. 204-230, 2011.

[10] A. Subramanian, U. Krishnan and S. Sethuraman, "Development of Biomaterial Scaffold for Nerve Tissue Engineering," *Journal of Biomedical Science,* vol. 16, no. 108, pp. 1-11, 2009.

[11] S. Jana, "PhD Thesis: Designing of Chitosan-Based Scaffolds for Biomedical," University of Washington, 2012.

[12] E. Biazar, M. Khorasani, . N. Montazeri and K. Poursham, "Types of Neural Guides and Using Nanotechnology for Peripheral Nerve Reconstruction Nondegradable Materials," *International Journal of Nanomedicine,* vol. 5, p. 839–852, 2010.

[13] L. Xue and H. Greisler, "Biomaterials in the development and future of vascular grafts," *Journal of Vascular Surgery,* vol. 32, no. 2, pp. 472-480, 2003.

[14] M. Siemionow, M. Bozkurt and F. Zor, "Regeneration and Repair of Peripheral Nerves with Different Biomaterials, Review," *Microsurgery,* vol. 30, no. 7, pp. 574-588, 2010.

[15] S. Geuna, S. Gnavi, I. Perrot, P. Tos and B. Battiston, "Tissue Engineering and Peripheral Nerve Reconstruction: An Overview," in *International Review of Neurobiology*, 1 ed., S. Geuna, I. Perroteau, P. Tos and B. Battiston, Eds., Elsevier Inc., 2013, pp. 35-57.

[16] P. Pranga, R. Müller, A. Eljaouhari, K. Heckmann, W. Kunz, T. Weber, C. Faber, M. Vroemen, U. Bogdahn and N. Weidner, "The promotion of oriented axonal regrowth in the injured spinal cord by alginate-based anisotropic capillary hydrogels," *Biomaterials*, vol. 27, p. 3560–3569, 2006.

[17] R. Muzzarelli, "Chitins and Chitosans as Immunoadjuvants and Non-Allergenic Drug Carriers," *Marine Drugs*, vol. 8, no. 2, p. 292–312, 2010.

[18] Y. Qiu, "PhD Thesis: Chitosan Derivatives for Tissue Engineering," Clemson University, 2008, pp. 4-5.

[19] A. Engesland, "Master Thesis: Hydrogels of Natural Origin in Wound Healing:

Formulation Devolpment," University of Tromsø, Department of Pharmacy, 2010, p. Chapter 1.

[20] C. Shi, Y. Zhu, X. Ran, M. Wang, Y. Su and T. Cheng, "Therapeutic potential of chitosan and its derivatives in regenerative medicine," *Journal of Surgical Research,* vol. 133, no. 2, pp. 185-192, 2006.

[21] B. Krajewska, "Application of chitin- and chitosan-based materials for enzyme immobilizations: a review," *Enzyme and Microbial Technology,* vol. 35, no. 2-3, 2004.

[22] C. Peniche,, W. Arguelles-Monal, H. Peniche and N. Acosta, "Chitosan: An attractive biocompatible polymer for microencapsulation," *Macromolecular Bioscience,* vol. 3, no. 10, pp. 511-520, 2003.

[23] I. Kim, , S. Seo, H. Moon, M. Yoo, I. Park, B. Kim and C. Cho, "Chitosan and its derivatives for tissue engineering applications," *Biotechnology Advances,* vol. 26, no. 1, pp. 1-21, 2008.

[24] M. Khorasani, H. Mirzadeh, A. Talebi and S. Irani, "Tubular scaffold design of polylactide acid for nerve tissue engineering: In-vitro," *4th European Conference of the International Federation for Medical and Biological Engineering,* vol. 22, pp. 2285-2287, 2009.

[25] G. Keilhoff, F. Stang, G. Wolf and H. Fansa, "Bio-compatibility of type I/III collagen matrix for peripheral nerve reconstruction," *Biomaterials,* vol. 24, no. 16, p. 2779–2787, 2003.

[26] F. Xie, Q. Li, B. Gu, K. Liu and G. Shen, "In vitro and in vivo evaluation of a biodegradable chitosan–PLA composite peripheral nerve guide conduit material," *Microsurgery,* vol. 28, no. 6, p. 471–479, 2008.

[27] Q. Wang, X. Yang, M. Ren, Y. Hu, Q. Chen, L. Xing, C. Meng and T. Liu, "Effect of chitosan/type I collagen/gelatin composites in biocompatibility and nerve repair," *Neural Regeneration Research,* vol. 7, no. 15, pp. 1179-1184, 2012.

[28] Z. Zheng, Y. Wei, G. Wang, Y. Gong and X. Zhang , "In vitro biocompatibility of

three chitosan/polycation composite materials for nerve regeneration," *Neural Regeneration Research,* vol. 3, no. 8, pp. 837-842, 2008.

[29] M. Meek, K. Jansen, R. Steendam, W. Oeveren, P. Wachem and M. Luyn, "In vitro degradation and biocompatibility of poly(DL-lactide-epsilon-caprolactone) nerve guides," *Journal of Biomedical Materials Research Part A,* vol. 68A, no. 1, p. 43–51, 2004.

[30] A. Wang, Q. Ao, Y. Wei, K. Gong, X. Liu, N. Zhao, Y. Gong and X. Zhang, "Physical properties and biocompatibility of a porous chitosan-based fiber-reinforced conduit for nerve regeneration," *Biotechnology Letters,* vol. 29, no. 11, pp. 1697-1702, 2007.

[31] S. Kehoe, X. Zhang and D. Boyd, "Composition–property relationships for an experimental composite nerve guidance conduit: evaluating cytotoxicity and initial tensile strength," *Journal of Materials Science: Materials in Medicine,* vol. 22, no. 4, pp. 945-959, 2011.

[32] S. Misra, S. Valappil, I. Roy and A. Boccaccini , "Polyhydroxyalkanoate (PHA)/Inorganic Phase Composites for Tissue Engineering Applications," *Biomacromolecules,* vol. 7, no. 8, pp. 2249-2258, 2006.

[33] A. Araújo, A. Lemos and J. Ferreira, "Rheological, microstructural, and in vitro characterization of hybrid chitosan-polylactic acid/hydroxyapatite composites," *Journal of Biomedical Materials Research Part A,* vol. 88A, no. 4, p. 916–922, 2009.

[34] C. Shen, Y. Yang, T. Huang, S. Chan and B. Liu, "Neural regeneration in a novel nerve conduit across a large gap of the transected sciatic nerve in rats with low-level laser phototherapy," *Journal of Biomedical Materials Research Part A,* vol. 101, no. 10, p. 2763–2777, 2013.

[35] C. Shen, Y. Yang, T. Huang, S. Chan and B. Liu, "Low-Level Laser-Accelerated Peripheral Nerve Regeneration within a Reinforced Nerve Conduit across a Large Gap of the Transected Sciatic Nerve in Rats," *Evidence-Based Complementary and Alternative Medicine,* vol. 2013, pp. 1-12, 2013.

[36] S. Bunting, L. Silvio, S. Deb and S. Hall, "Bioresorbable Glass Fibres Facilitate Peripheral Nerve Regeneration," *The Journal of Hand Surgery: British & European Volume,* vol. 30, no. 3, p. 242–247, 2005.

[37] S. Caridade , E. Merino , N. Alves and J. Mano, "Biomineralization in chitosan/Bioglass® composite membranes under different dynamic mechanical conditions," *Materials Science and Engineering: C,* vol. 33, no. 7, pp. 4480-4483, 2013.

[38] P. Gentile, M. Belmonte, V. Chiono, C. Ferretti, F. Baino, C. Turo, C. Brovarone, I. Pashkuleva, R. Reis and G. Ciardelli, "Bioactive glass/polymer composite scaffolds mimicking bone tissue," *Journal of Biomedical Materials Research Part A,* vol. 100A, no. 10, p. 2654–2667, 2012.

[39] J. Zheng, "Turning of nerve growth cones induced by localized increases in intracellular calcium ions," *Nature,* vol. 403, pp. 89-93, 2000.

[40] S. Kater SB and L. Mills, "Regulation of growth cone behaviour by calcium," *The Journal of Neuroscience,* vol. 11, no. 4, pp. 891-899, 1991.

[41] J. Henley and M. Poo, "Guiding neuronal growth cones using Ca2+ signals," *Trends in Cell Biology,* vol. 14, no. 6, p. 320–330, 2004.

[42] B. Ünal, H. Tan, Z. Orbak, L. Kiki, M. Bilici, N. Bilici, H. Aslan and S. Kaplan, "Morphological alteration produced by zinc deficiency in rat sciatic nerve: a histological, electron microscope, and stereological study," *Brain Research,* vol. 1048, no. 1-2, pp. 228-234, 2005.

[43] D. Boyd, H. Li, D. Tanner, M. Towle and J. Wall, "The antibacterial effects of zinc ion migration from zinc-based glass polyalkenoate cements," *Journal of Materials Science: Materials in Medicine,* vol. 17, no. 6, pp. 489-494, 2006.

[44] X. Zhang , S. Kehoe, S. Adhi, T. Ajithkumar, S. Moane, H. O'Shea and D. Boyd, "Composition-structure-property (Zn2+ and Ca2+ Ion release) evaluation of Si-Na-Ca-Zn-Ce glasses: potential components for nerve guidance conduits," *Materials Science and Engineering: C,* vol. 31, no. 3, pp. 669-676, 2011.

[45] A. Goel, S. Kapoor, A. Tilocca, R. Rajagopal and J. Ferreira, "Structural role of zinc in biodegradation of alkali-free bioactive glasses," *Journal of Materials Chemistry B*, vol. 1, no. 24, p. 3073–3082, 2013.

[46] L. Bi, S. Jung, D. Day, K. Neidig K, V. Dusevich and D. Eick, "Evaluation of bone regeneration, angiogenesis, and hydroxyapatite conversion in critical-sized rat calvarial defects implanted with bioactive glass scaffolds," *Journal of Biomedical Materials Research Part A*, vol. Volume 100A, no. 12, p. 3267–3275, 2012.

[47] I. Farooq, Z. Imran, U. Farooq, A. Leghari and H. Ali, "Bioactive glass, a material for the future," *World Journal of Dentistry*, vol. 3, no. 2, pp. 199-201, 2012.

[48] R. Hill and M. Stevens, "Bioactive Glass". Patent U.S. 20090208428-A1, 2009.

[49] X. Dai, L. Wang, K. Ma, B. Liu, H. Li and K. Pan, "Characterization of a Hybridization Scaffold Based on PLGA/Acellular Pigskin for Nerve Regeneration," *Journal of Medical and Biological Engineering*, vol. 33, no. 2, pp. 221-228, 2013.

[50] J. Zhu, Y. Xiong, C. Zeng, N. Qiang and J. Wan, "Elastic chitosan conduits with multiple channels and well defined microstructure," *International Journal of Biological Macromolecules*, vol. 51, no. 1-2, pp. 105-112, 2012.

[51] Y. Wei, K. Gong, Z. Zheng, A. Wang, Q. Ao, Y. Gong and X. Zhang, "Chitosan/silk fibroin-based, Schwann cell-derived extracellular matrix-modified scaffolds for bridging rat sciatic nerve gaps," *Journal of Materials Science: Materials in Medicine*, vol. 22, no. 8, pp. 1947-1964, 2011.

[52] C. Liao, F. Zhang, R. Guo, X. Zhong, J. Zhu, X. Wen and J. Shen, "Peripheral Nerve Repair: Monitoring by Using Gadofluorine M–enhanced MR Imaging with Chitosan Nerve Conduits with Cultured Mesenchymal Stem Cells in Rat Model of Neurotmesis," *Radiology*, vol. 262, no. 1, pp. 161-171, 2012.

[53] R. Muzzarelli, "Biomedical exploitation of chitin and chitosan via mechano-chemical disassembly, electrospinning, dissolution in imidazolium ionic liquids, and supercritical drying," *Marine Drugs*, vol. 9, no. 9, pp. 1510-1533, 2011.

[54] X. Wang, W. Hu, Y. Cao, J. Yoa, J. Wu and X. Gu, "Dog sciatic nerve regeneration

across a 30-mm defect bridged by a chitosan/PGA artificial nerve graft," *Brain,* vol. 128, no. 8, pp. 1897-1910, 2008.

[55] B. Hoffmann, D. Seitz, A. Mencke, A. Kokott and G. Ziegler, "Glutaraldehyde and Oxidized Dextran As Crosslinker Reagents for Chitosan-based Scaffolds for Cartilage Tissue Engineering," *Journal of Materials Science: Materials in Medicine,* vol. 20, no. 7, pp. 1495-1503, 2009.

[56] F. Mi, H. Sung and S. Shyu, "Synthesis and Characterization of a Novel Chitosan-based Network Prepared Using Naturally Occurring Crosslinker," *Journal of Polymer Science, Part A: Polymer Chemistry,* vol. 38, no. 15, pp. 2804-2814, 2000.

[57] Y. Li, T. Liu, J. Zheng and X. Xu, "Glutaraldehyde-crosslinked chitosan/hydroxyapatite bone repair scaffold and its application as drug carrier for icariin," *Journal of Applied Polymer Science,* vol. 130, no. 3, pp. 1539-1547, 2013.

[58] S. Grieshaber, A. Jha, A. Farran and X. Jia, "Hydrogels in Tissue Engineering," in *Biomaterials for Tissue Engineering Applications: A Review of the Past and Future Trends*, New York, Springer-Verlag/Wien, 2011, pp. 16-17.

[59] F. Mi, S. Shyu and C. Peng, "Characterization of Ring-Opening Polymerization of Genipin and pH-Dependent Cross-Linking Reactions Between Chitosan and Genipin," *Journal of Polymer Science, Part A: Polymer Chemistry,* vol. 43, no. 10, pp. 1985-2000, 2005.

[60] J. Jin, M. Song and D. Hourston, "Novel Chitosan-Based Films Cross-Linked by Genipin with Improved Physical Properties," *Biomacromolecules,* vol. 5, no. 1, pp. 162-168, 2004.

[61] C. Tsai, R. Huang, H. Sung and H. Liang, "In vitro evaluation of the genotoxicity of a naturally occurring crosslinking agent (genipin) for biologic tissue fixation," *Journal of Biomedical Materials Research,* vol. 52, no. 1, p. 58–65, 2000.

[62] F. Mi, Y. Tan, H. Liang, R. Huang and H. Sung, "In vitro evaluation of a chitosan membrane cross-linked with genipin," *Journal of Biomaterials Science, Polymer Edition,* vol. 12, no. 8, pp. 835-850, 2001.

[63] V. Chiono, E. Pulieri, G. Vozzi and G. Ciardelli, "Genipin-Crosslinked chitosan/gelatin blends for biomedical applications," *Journal of Materials Science: Materials in Medicine,* vol. 19, no. 2, pp. 889-898, 2008.

[64] H. Sung , Y. Chang, C. Chiu and C. Chen, "Crosslinking characteristics and mechanical properties of a bovine pericardium fixed with a naturally occurring crosslinking agent," *Journal of Biomedical Materials Research,* vol. 47, no. 2, pp. 116-126, 1999.

[65] H. Hosseinkhani and M. Hosseinkhani, "Tissue Engineered Scaffolds for Stem Cells and Regenerative Medicine," in *Trends in Stem Cell Biology and Technology,* H. Baharvand, Ed., Humana Press, 2009, p. Chapter 19.

[66] T. Cui, Y. Yan, R. Zhang and X. Wang, "Biomodeling and fabricating of a Hybrid PU Collagen Nerve Regeneration Conduit," *IEEE International Conference on Virtual Environments, Human-Computer Interfaces, and Measurements Systems,* pp. 79-84, 2009.

[67] H. Zhang and A. Cooper, "Aligned Porous Structures by Directional Freezing," *Advanced Materials,* vol. 19, no. 11, p. 1529–1533, 2007.

[68] E. Kijeńska, M. Prabhakaran, W. Swieszkowski, K. Kurzydlowski and S. Ramakrishna, "Electrospun Bio-Composite P(LLA-CL)/Collagen I/Collagen III Scaffolds for Nerve Tissue Engineering," *Journal of Biomedical Materials Research Part B: Applied Biomaterials,* vol. 100B, no. 4, p. 1093–110, 2012.

[69] H. Chung and T. Park , "Surface Engineered and Drug Releasing Pre-Fabricated Scaffolds for Tissue Engineering," *Advanced Drug Delivery Reviews,* vol. 59, no. 4-5, p. 249–262, 2007.

[70] S. Suri, L. Han, W. Zhang, A. Singh, S. Chen and C. Schmidt, "Solid freeform fabrication of designer scaffolds of hyaluronic acid for nerve tissue engineering," *Biomedical Microdevices,* vol. 13, no. 6, pp. 983-993, 2011.

[71] H. Ke, Master Thesis: Investigation into The Dispensing–Based Fabrication Process For Tissue Scaffolds, Department of Mechanical Engineering , University of

Saskatchewan, Saskatoon, 2006, p. 13.

[72] L. Bi, Z. Cao, Y. Hu, Y. Song, L. Yu, B. Yang, J. Mu, Z. Huang and Y. Han, "Effects of different cross-linking conditions on the properties of genipin-cross-linked chitosan/collagen scaffolds for cartilage tissue engineering," *Journal of Materials Science: Materials in Medicine,* vol. 22, no. 1, pp. 51-62, 2011.

[73] L. Yan, Y. Wang, L. Ren, G. Wu, S. Caridade, J. Fan, L. Wang, P. Ji, J. Oliveira, J. Oliveira, J. Mano and R. Reis, "Genipin-cross-linked collagen/chitosan biomimetic scaffolds for articular cartilage tissue engineering application," *Journal of Biomedical Materials Research Part A,* vol. 95A, no. 2, pp. 465-475, 2010.

[74] B. Yang, X. Li, S. Shi, X. Kong, G. Guo, M. Huang, F. Luo, Y. Wei, X. Zhao and Z. Qian, "Preparation and characterization of a novel chitosan scaffold," *Carbohydrate Polymers,* vol. 80, no. 3, p. 860–865, 2010.

[75] P. Datta, G. Thakur, J. Chatterjee and S. Dharad, "Biofunctional Phosphorylated Chitosan Hydrogels Prepared Above pH 6 and Effect of Crosslinkers on Gel Properties Towards Biomedical Applications," *Soft Materials,* vol. 12, no. 1, pp. 27-35, 2014.

[76] S. Dehghani, B. Rahmanifar , A. Moradi and P. Azar, "Removal of permethrin pesticide from water by chitosan–zinc oxide nanoparticles composite as an adsorbent," *Journal of Saudi Chemical Society,* vol. in Press, 2014.

[77] M. Rhazi, J. Desbrières, A. Tolaimate, M. Rinaudo, P. Vottero, A. Alagui and M. El Meray, "Influence of the nature of the metal ions on the complexation with chitosan.," *European Polymer Journal,* vol. 38, no. 8, p. 1523–1530, 2002.

[78] I. Kansal , A. Goel, D. Tulyaganov, R. Rajagopal and J. Ferreira, "Structural and thermal characterization of CaO–MgO–SiO2–P2O5–CaF2 glasses," *Journal of the European Ceramic Society,* vol. 32, no. 11, p. 2739–2746, 2012.

[79] M. Sarem , F. Moztarzadeh and M. Mozafari, "How can genipin assist gelatin/carbohydrate chitosan scaffolds to act asreplacements of load-bearing soft tissues," *Carbohydrate Polymers,* vol. 93, no. 2, p. 635–643, 2013.

[80] N. Kil'deeva, P. Perminov, L. Vladimirov, V. Novikov and S. Mikhailov, "About Mechanism of Chitosan Cross-Linking with Glutaraldehyde," *Russian Journal of Bioorganic Chemistry,* vol. 35, no. 3, pp. 360-369, 2009.

[81] K. Chen, "Asymmetric Chitosan Membrane Containing Collagen I Nanospheres for Skin Tissue Engineering," *Biomacromolecules,* vol. 10, no. 6, pp. 1642-1649, 2009.

[82] G. Gorczyca , R. Tylingo, P. Szweda, E. Augustin, M. Sadowska and S. Milewski, "Preparation and characterization of genipin cross-linked porous chitosan–collagen–gelatin scaffolds using chitosan–CO2 solution," *Carbohydrate Polymers,* vol. 102, p. 901–911, 2014.

[83] C. Yao, B. Liu, C. Chang, S. Hsu and Y. Chen, "Preparation of networks of gelatin and genipin as degradable biomaterials," *Materials Chemistry and Physics,* vol. 83, no. 2-3, p. 204–208, 2004.

[84] H. Chen, W. Ouyang, B. Lawuyi, C. Martoni and S. Prakash, "Reaction of chitosan with genipin and its fluorogenic attributes for potential microcapsule membrane characterization," *Journal of Biomedical Materials Research Part A,* vol. 75A, no. 4, pp. 917-927, 2005.

[85] L. Damink, P. Dijkstra, M. Luyn, P. Wachem, P. Nieuwenhuis and J. Feijen, "Glutaraldehyde as a crosslinking agent for collagen-based biomaterials," *Journal of Materials Science: Materials in Medicine,* vol. 6, no. 8, pp. 460-472, 1995.

[86] O. Monteiro Jr and C. Airoldi, "Some studies of crosslinking chitosan–glutaraldehyde interaction in a homogeneous system," *International Journal of Biological Macromolecules,* vol. 26, no. 2-3, p. 119–128, 1999.

[87] R. Muzzarelli, "Genipin-crosslinked chitosan hydrogels as biomedical and pharmaceutical aids," *Carbohydrate Polymers,* vol. 77, no. 1, p. 1–9, 2009.

[88] Y. Shirosaki , T. Okayama, K. Tsuru, S. Hayakawa and A. Osaka, "Synthesis and cytocompatibility of porous chitosan–silicate hybrids for tissue engineering scaffold application," *Chemical Engineering Journal,* vol. 137, no. 1, p. 122–128, 2008.

[89] L. Ren, K. Tsuru , S. Hayakawa and A. Osaka, "Sol–gel preparation and in vitro

deposition of apatite on porous gelatin–siloxane hybrids," *Journal of Non-Crystalline Solids,* vol. 285, no. 1-3, p. 116–122, 2001.

[90] H. Kang , Y. Tabata and W. Ikada, "Fabrication of porous gelatin scaffolds for tissue engineering," *Biomaterials,* vol. 20, no. 14, p. 1339–1344, 1999.

[91] M. Ho, P. Kuo, H. Hsieh, T. Hsien, L. Huo, J. Lai and D. Wang, "Preparation of porous scaffolds by using freeze-extraction and freeze-gelation methods," *Biomaterials,* vol. 25, no. 1, p. 129–138, 2004.

[92] X. Gu, F. Ding, Y. Yang and J. Liu, "Construction of tissue engineered never grafts and their application in peripheral never regeneration," *Progress in Neurobiology,* vol. 93, no. 2, p. 204–230, 2011.

[93] W. Daly, L. Yao, D. Zeugolis, A. Windebank and A. Pandit, "A biomaterials approach to peripheral nerve regeneration: bridging the peripheral nerve gap and enhancing functional recovery," *Journal of the Royal Society Interface,* vol. 9, no. 67, p. 202–221, 2012.

[94] B. Hoffmann, D. Seitz, A. Mencke, A. Kokott and G. Ziegler, "Glutaraldehyde and oxidised dextran as crosslinker reagents for chitosan-based scaffolds for cartilage tissue engineering," *Journal of Materials Science: Materials in Medicine,* vol. 20, no. 7, pp. 1495-1503, 2009.

[95] S. Amado, M. Simões , P. Silva , A. Luís, Y. Shirosaki, M. Lopes, J. Santos, F. Fregnan, G. Gambarotta, S. Raimondo, M. Fornaro, A. Veloso, A. Varejão, A. Maurício and S. Geuna, "Use of hybrid chitosan membranes and N1E-115 cells for promoting nerve regeneration in an axonotmesis rat model," *Biomaterials,* vol. 29, no. 33, p. 4409–4419, 2008.

[96] Y. Wan, J. Huang, J. Zhang, D. Yin, Z. Zheng , C. Liao and S. Sun, "Investigation of mechanical properties and degradability of multi-channel chitosanepolycaprolactone/collagen conduits," *Polymer Degradation and Stability,* vol. 98, no. 1, p. 122–132, 2013.

[97] H. Wu , Y. Wan , X. Cao and Q. Wu, "Proliferation of chondrocytes on porous

poly(dl-lactide)/chitosan scaffolds," *Acta Biomaterialia,* vol. Volume 4, no. 1, p. 76–87, 2008.

[98] M. Kon and A. Visser, "A poly (HEMA) sponge for restoration of articular cartilage defects," *Plastic & Reconstructive Surgery,* vol. 67, no. 3, pp. 289-293, 1981.

[99] R. Tığlı and M. Gümüşderelioğlu, "Evaluation of alginate-chitosan semi IPNs as cartilage scaffolds," *Journal of Materials Science: Materials in Medicine,* vol. 20, no. 3, pp. 699-709, 2009.

[100] Y. Wei, K. Gong, Z. Zheng and A. Wang, "Chitosan/silk fibroin-based tissue-engineered graft seeded with adipose-derived stem cells enhances nerve regeneration in a rat model," *Journal of Materials Science: Materials in Medicine,* vol. 22, no. 8, pp. 1947-1964, 2011.

[101] Y. Yuan, B. Chesnutt, G. Utturkar, W. Haggard, Y. Yang, J. Ong and J. Bumgardner, "The effect of cross-linking of chitosan microspheres with genipin on protein release," *Carbohydrate Polymers,* vol. 68, no. 3, p. 561–567, 2007.

[102] M. Haugh, "The Development of Novel Scaffolds for Tissue Engineering with a Range of Structural and Mechanical Properties," in *PhD Thesis,* Trinity College, 2009.

[103] S. Güven, "Integrated Biomimetic Scaffolds for Soft Tissue Engineering," in *Master Thesis,* Middle East Technical University, School of Natural and Applied Sciences, 2006, p. Chapter 1.

[104] L. Pfister, M. Papaloïzos, H. Merkle and B. Gander, "Nerve Conduits and Growth Factor Delivery in Peripheral Nerve Repair," *Journal of the Peripheral Nervous System,* vol. 12, no. 2, pp. 65-82, 2007.

[105] X. Wang, Y. Du, L. Fan, H. Liu and Y. Hu, "Chitosan-metal complexes as antimicrobial agent: Synthesis, characterization and Structure-activity study," *Polymer Bulletin,* vol. 55, no. 1-2, p. 105–113, 2005.